CHARACTERIZATION BY ^{15}N-METABOLIC LABELING AND MASS SPECTROMETRY OF PROTEINS FOR HIGH-LIGHT ADAPTATION IN *SYNECHOCOCCUS* SP. PCC 7002 CYANOBACTERIA

By Jessica M. Dorschner

The marine cyanobacterium *Synechococcus* sp. PCC 7002 tolerates extreme high-light intensities of more than twice full sunlight (≥2000 μmol photons m^{-2} s^{-1}), a stress condition that can damage cellular machinery via the production of reactive oxygen species (ROS). While many cyanobacterial photoprotective mechanisms have been identified to mitigate ROS-induced damage, quantification of the protein response of *Synechococcus* sp. PCC 7002 to extreme high light intensity may contribute to our understanding of these processes.

^{14}N- and ^{15}N-metabolic labeling of *Synechococcus* sp. PCC 7002 cultures, coupled with electrospray (ESI)-Ion trap and MALDI-TOF mass spectrometry (MS) analyses of the tryptic peptides, were employed to quantify protein levels in response to high- versus optimal-light intensity. The ESI-Ion trap mass spectrometer provided tandem, fragmentation (MS^2) mass/charge (*m/z*) lists that were searched against a custom MASCOT database to identify the ^{14}N and ^{15}N peptide sequences.

Optimization of the ESI-Ion trap MS parameters increased the total number of compounds and protein identifications by ~2-fold. Separation of the soluble protein fraction into SDS-PAGE gel-band digests resulted in a similar number of ESI-Ion trap MS protein identifications (IDs) as the bulk digest (29 vs 28). However, the separate gel-band MS analyses resulted in 19 additional unique protein IDs.

Both ^{14}N-high- and ^{15}N-optimal-light peptides were detected by ESI-Ion trap MS, and showed characteristic *m/z* mass shifting due to the ^{14}N (light) versus ^{15}N (heavy) isotopic incorporation. Some of these ^{14}N-high- and ^{15}N-optimal-light peptides were cross-detected by MALDI-TOF mass spectrometry for relative protein quantification analyses. Phycobilisome light harvesting proteins and membrane-fraction photosystem protein were predominantly detected, and levels decreased 2-fold under high-light intensity.

Work presented here demonstrate that downregulation of light-harvesting and photosynthesis proteins is part of the adaptive mechanism that allows *Synechococcus* sp. PCC 7002 to thrive at high light intensities. Furthermore, ^{15}N-metabolic labeling of *Synechococcus* 7002 cells by substituting ^{15}N-$NaNO_3$ in the growth medium in place of ^{14}N-$NaNO_3$ is a simple and effective strategy for isotopic labeling of proteins for quantitative mass spectrometry.

CHARACTERIZATION BY ^{15}N-METABOLIC LABELING AND MASS SPECTROMETRY OF PROTEINS FOR HIGH-LIGHT ADAPTATION IN *SYNECHOCOCCUS* SP. PCC 7002 CYANOBACTERIA

by

Jessica M. Dorschner

A Thesis Submitted
In Partial Fulfillment of the Requirements
For the Degree of

Masters of Science – Biology

Microbiology

at

The University of Wisconsin Oshkosh
Oshkosh WI 54901-8621

May 2018

COMMITTEE APPROVAL

Advisor

2/2/2018 Date Approved

Member

2/2/18 Date Approved

Member

2/2/18 Date Approved

PROVOST & VICE CHANCELLOR

June 1, 2018
Date Approved

FORMAT APPROVAL

6/12/18
Date Approved

TABLE OF CONTENTS

LIST OF TABLES

LIST OF FIGURES

Introduction

Cyanobacteria hold great evolutionary significance as the original producers of atmospheric oxygen and ancestors of chloroplasts in eukaryotic algae and plants. They can be found in nearly every type of habitat, and continue to contribute to global ecological carbon, oxygen, and nitrogen cycling. Cyanobacterial cells contain internal photosynthetic membranes. They have minimal growth requirements, thriving on only light, CO_2, and simple inorganic nutrients. Cyanobacteria are excellent model organisms for studying photosynthesis, prokaryotic circadian rhythms, and as hosts for production of carbon-neutral bioproducts and biofuels.

The marine cyanobacterium *Synechococcus* sp. PCC 7002 (hereafter *Synechococcus* 7002) tolerates a wide range of salt conditions [1], is amenable to genetic manipulation [2, 3], and is among the fastest-growing of any photosynthetic organisms. Interestingly, *Synechococcus* 7002 can withstand extreme high light intensities of more than twice full sunlight with very little change in growth rate [4]. Other laboratory strains of cyanobacteria, such as *Synechocystis* sp. 6803, experience impaired growth and bleaching under similar high light intensity conditions.

Exposure to high light intensities of full sunlight ($\geq$2000 μmol photons m^{-2} s^{-1}) is a common stress condition faced by many photosynthetic organisms, causing damage to cellular machinery via production of reactive oxygen species (ROS) [5]. Many photoprotective mechanisms have been identified in cyanobacteria, including: dissipation of excess light energy as heat by carotenoids [6] [7], conversion of ROS to O_2 or H_2O_2 by

enzymes such as superoxide dismutase [8], photoreduction of excess O_2 by A-type flavoproteins [9], and modulation of the redox state of the photosynthetic electron transport chain (*e.g.*, via state transitions of the light harvesting antenna complexes [10], formation of nonfunctional photosystem II complexes [11] [12], and cytosolic redox regulators such as thiol tripeptides [13, 14]). These photoprotective processes, along with potential undiscovered mechanisms, may be particularly interesting in the extremely high light tolerant *Synechococcus* 7002.

A recent study found substantial differential regulation of *Synechococcus* 7002 genes and proteins in response to high light stress, including photosynthesis pathways, resistance to light-induced damage, DNA replication and repair, and energy metabolism [15]. Trypsin digestion of extracted proteins coupled with tandem mass spectrometry (MS/MS) was employed for their proteomic analyses. The high sensitivity and throughput of mass spectrometry (MS) make it an excellent proteomics methodology; however, quantification can be challenging, because peptides have variable signal intensities within the mass spectrometer because of their differing amino acid sequences. A given peptide may have a high MS signal intensity simply because its amino acid sequence chemistry results in more efficient ionization within the instrument – not because it is biologically more abundant. There are a few ways to circumvent this MS signal intensity problem for peptide and thus protein quantification, such as automated spectral counting of peptide ions [16], or as in the *Synechococcus* 7002 proteomics study of Xiong *et al.* [15], isobaric tandem mass tagging (TMT) of the tryptic peptides prior to mass spectrometry [17]. TMT reagents contain an NH_2-reactive group that binds to the

peptides, a mass normalizer group that allows for isobaric multiplexing, and a mass reporter group [18]. The mass reporter group is cleaved during the peptide fragmentation step within the mass spectrometer, allowing for detection and relative quantification of the differential isotopic peaks during the tandem MS/MS analyses. The downside of TMT-quantification is that it requires significant peptide processing steps prior to MS, relying on mass tagging efficiency and consistency between samples, to prevent introducing additional, unwanted experimental variation.

An alternative MS-quantification method is to metabolically-incorporate stable, isotopic ^{15}N directly into microbial cultures – in this case *Synechococcus* 7002 cells, by substituting the sole nitrogen source in the growth medium ($NaNO_3$) with manufactured ^{15}N-$NaNO_3$ instead of the natural form of $NaNO_3$ (>98% ^{14}N-enriched). Thus, *Synechococcus* cells grown in ^{15}N medium synthesize amino acids and proteins that are labeled with ^{15}N, whereas cells grown in native ^{14}N medium synthesize ^{14}N amino acids and proteins. With this approach, *Synechococcus* cultures exposed to different conditions, such as high vs optimal light intensity, can be grown in separate ^{14}N vs ^{15}N media. These harvested cultures can then be mixed based on equal cell numbers, and subjected to concomitant processing for MS (cell lysis, fractionation, proteolysis by trypsin digestion, peptide desalting, and instrumental analysis), thus reducing experimental variation during the post-culture, pre-MS steps. Matched $^{14}N/^{15}N$ variants of the same peptides from these culture mixtures are distinguishable because their MS signals show predictable isotopic mass shifts. Because the amino acid sequences and chemistries of these matched peptides are the same, their ionization efficiencies are the same and their signal intensity ratios

provide accurate relative quantification. These methods have been successfully demonstrated for a number of microorganisms including the halotolerant cyanobacterium *Euhalothece* sp. BAA001, providing relative MS protein quantification between different saline conditions [19]. ^{15}N stable isotope metabolic labeling is easily applicable to cyanobacteria such as *Synechococcus* 7002 and *Euhalothece* sp. BAA001, because they do not fix/incorporate atmospheric nitrogen, and can be grown in simple, defined saltwater media. Currently, ^{15}N metabolic labeling of *Synechococcus* 7002 has been conducted for MS metabolite profiling, but not for proteomics [20]. Herein, $^{14}N/^{15}N$ metabolic labeling, coupled with trypsin digestion and tandem mass spectrometry, was employed with *Synechococcus* 7002 to compare relative protein expression under an optimal light intensity of 200 µmol photons m^{-2} s^{-1} that already saturates photosynthesis vs extreme high-light intensity of 2000 µmol photons m^{-2} s^{-1} that is lethal to many microalgae. The goal of this study was to identify proteins or protein regulation that may have roles in adaptation to extreme, high-light intensity.

Methods

Synechococcus 7002 Cultures and Metabolic Labeling

Two stock cultures of *Synechococcus* 7002 were maintained under ambient light, temperature, and mild agitation, with one flask containing ^{14}N-$NaNO_3$ to fulfill the A^+ medium recipe [2] and the other containing heavy isotopic nitrate ^{15}N-$NaNO_3$. The ^{15}N stock culture was grown for at least eight generations and transferred twice to fresh ^{15}N medium prior to experimental runs to ensure thorough ^{15}N metabolic incorporation. These stock cultures were used to inoculate experimental Roux bottles of 300ml A^+ medium (either ^{14}N or ^{15}N media), which were grown at 37°C with constant stirring and 3% CO_2/air flow. The ^{15}N Roux cultures were grown under optimal light (200 µmol photons m^{-2} s^{-1}) until the culture optical cell density ($O.D._{750nm}$ cm^{-1}, hereafter $O.D._{750}$) reached 0.5 (mid-exponential phase of culture growth). The ^{14}N Roux cultures were grown under the same optimal light intensity until they reached a cell density of $O.D._{750}$ = 0.2, at which point they were subjected to high light intensity (2000 µmol photons m^{-2} s^{-1}) until they reached an $O.D._{750}$ of 0.5, resulting in a 2 h exposure to high light prior to harvest at the mid-exponential growth phase. In short, **^{14}N cultures = high light exposure** (for 2 h prior to harvest), **^{15}N cultures = optimal light exposure**.

Cell Harvest and Lysis for Protein Analysis

100 ml of each Roux bottle culture ($O.D._{750}$ = 0.5) was pelleted and washed twice with 5mM HEPES-NaOH pH 7.5 buffer. The washed cell pellets were stored at -80°C until used for analysis. Five ml of each culture was also harvested for cell counting and pelleted for archival at -80°C for subsequent chlorophyll and/or protein quantification assays.

Prior to the cell lysis, two of the washed pellets (one from a ^{14}N-high light culture and one from a ^{15}N-optimal light culture) were thawed, resuspended in the 5 mM HEPES-NaOH pH 7.5 buffer, and mixed according to equal cell numbers to obtain a 10 ml volume. Three biological replicates of these 10 ml $^{14}N/^{15}N$ cell mixtures were used for all downstream sample processing and mass spectrometry analyses. A protease inhibitor cocktail (0.5 mM Pefabloc , 1 mM amino-caproic acid, 1 mM benzamidine, 1 µM pepstatin A, 10 µM leupeptin, 1 µM E-64, 1 µM bestatin), 2 mM dithiothreitol (DTT), and 30 µg/ml DNase were also included in the 10 ml mixed protein samples.

The 10 ml mixed $^{14}N/^{15}N$ cell suspensions were sheared slowly (~1 drop per s) by passage through an ice-cold pressurized, French press cylinder (20,000 psi) three times to achieve cell lysis. The resultant lysates were clarified by centrifugation (10 min, 6000 x *g*) to pellet the cell wall debris, and the cleared lysates ultracentrifuged (1 h, 184,000 x *g*, 4°C) to obtain two protein fractions: the soluble protein supernatant and pellet containing membrane vesicles and membrane proteins. The membrane proteins were resuspended in 1 ml of the HEPES buffer, and both the membrane (mp) and soluble (sp) fractions were stored at -80°C until used for analyses.

Bulk Trypsin Digestion of Soluble Proteins

The soluble protein (sp) samples were precipitated by addition of acetone to 80% and incubated at -20°C for 30 min, followed by centrifugation (15,000 x *g*, 4°C, 15 min) to obtain a concentrated protein pellet. 400 µg of this concentrated pellet was resuspended to 16 mg protein/ml in 8 M urea, 10 mM dithiothreitol (DTT), 100 mM Na phosphate pH 7.0 buffer and incubated at 30°C for 30 min with intermittent vortexing to facilitate protein denaturation. Samples were then diluted 8-fold prior to addition of trypsin (1:50 trypsin:protein *w/w*, Promega) and incubated overnight at 37°C with gentle rocking. Formic acid was added to 5% (*v/v*) to quench the trypsin digestion, followed by purification/desalting with Varian Spec PT C18 pipette tip columns. The resultant tryptic peptides were suspended to 1 µg/µl in 0.3% formic acid in preparation for high performance liquid chromatography – electrospray ionization – tandem mass spectrometry (HPLC-ESI-MS/MS).

Sodium Dodecyl Sulfate Polyacrylamide Gel Electrophoresis (SDS-PAGE) and In-gel Trypsin Digestion

Pre-cast SDS-PAGE gels (ThermoScientific Precise™, 4-20% acrylamide, 10-well) and a BioRad Mini-Protean 3 electrophoresis system were used to resolve the membrane and soluble proteins, according to the manufacturer's instructions, with the

following exceptions: 1) 250 µg of protein was overloaded per lane to maximize downstream output of trypsin-digested peptides, 2) the membrane protein (mp) gel loading buffer was adjusted to 4% SDS to facilitate solvation of the hydrophobic membrane proteins and centrifuged prior to loading (30 min at maximum speed in a microcentrifuge, ~12,000 x *g*) to sediment unsolubilized proteins and vesicles, and 3) the mp gel was run slowly overnight (at 10 V) as opposed to the standard 1 h (110-120V). Additionally, the soluble proteins were acetone-precipitated as described above and the membrane proteins were pelleted (centrifuged at maximum speed in a microcentrifuge for 12 mins, ~12,000 x *g*, 4°C) before resuspension with the gel loading buffer. The resultant gels were stained with freshly prepared, MS-compatible "blue silver" Coomassie [21].

The sp and mp gels were excised according to approximate molecular weight (kD), as determined by the Biorad Precision Plus Protein™ Prestained standard lanes. The sp gels were cut into seven bands: 10-15, 15-20, 20-37, 37-50, 50-75, 75-100, and 100-250 kD, and the mp gel was cut into six bands: <20, 20-37, 37-55, 55-100, 100-250, and ≥250 kD. The gels from different replicate cultures were treated similarly to provide separate biological replicates.

The gel slices were minced into small 1 x 1 mm pieces and destained by washing twice with 50% acetonitrile (ACN), 50% 5 mM NH_4HCO_3 for a total of 5 h, followed by a 2 min dehydration with 100% ACN. The gel pieces were rehydrated in 15 mM DTT, 5 mM NH_4HCO_3 for 40 min at 56°C. The DTT solution was removed, and the gel pieces

were protected from light and incubated with 55 mM iodoacetamide, 5 mM NH_4HCO_3 for 30 min. Finally, the gel pieces were dehydrated briefly with 100% ACN and rehydrated in a minimal volume (30 µl per microfuge tube—just enough to rehydrate and cover the gel pieces) of 12.5 ng/µl trypsin, 5 mM NH_4HCO_3. The samples were topped with 80 µl of NH_4HCO_3 buffer, and allowed to digest for 16-24 h at 37°C with gentle rocking.

The peptide digests were desalted using Omix C18 100 µl tips and resuspended in 35 µl of 0.3% formic acid in preparation for HPLC-ESI-MS/MS.

HPLC ESI-Ion Trap MS/MS

10 µl of each peptide digest was subjected to high-performance liquid chromatography (reverse-phased, 0.3 x 50mm Agilent Zorbax C18 column, phase A = 0.1% formic acid, phase B = 90% ACN, 0.1% formic acid) at a flow rate of ~3 µl/min for 145 min coupled to a Bruker Esquire™ 3000*plus* electrospray ion trap mass spectrometer. The standard instrument parameters for mass spectrometry included automated ion selection, collision-induced dissociation (CID), and tandem ion-trap mass spectrometry (MS/MS). Mass/charge (*m/z*) lists of the CID MS/MS spectra were searched against an in-house, custom MASCOT database for *Synechococcus* sp. PCC 7002 to identify peptide amino acid sequences and corresponding proteins. Because of instrument problems that arose during the thesis research, only one biological replicate of each gel slice was subjected to this HPLC ESI-ion trap MS/MS.

MALDI-TOF MS

All three biological replicates of each gel slice (39 samples total) were analyzed via matrix-assisted laser desorption ionization-time of flight (MALDI-TOF) MS. First, each desalted, in-gel peptide digest was mixed 1:1 with freshly prepared α-cyano-4-hydroxycinnamic acid (at 7 mg/ml in 70% ACN, 0.1% trifluoroacetic acid). 2 µl droplets of each sample mixture were allowed to air dry/crystallize on a stainless steel sample target plate. The MALDI-TOF instrument (Bruker Reflex IV) parameters included reflectron mode, laser intensity of 42-45, detector gain of 3.6-4.3, and 200 cumulative laser shots. Calibration was performed using Bruker Peptide Standards. Bruker FlexAnalysis software and paired t-tests were used for the quantitative peak area comparisons.

Results

Optimization of HPLC ESI-Ion Trap MS/MS Parameters for Increased Bulk Soluble Protein Identifications

To identify trypsin-digested *Synechococcus* 7002 peptide ions, mass/charge (*m/z*) lists from the tandem, fragmented (MS^2) ions were searched against a custom MASCOT *Synechococcus* sp. PCC 7002 peptide database. The HPLC-ESI-Ion trap mass spectrometer used for the MS^2 analyses has numerous parameters, including the HPLC flow rate (in µl/min), Ion trap Target size (ranges from ~10,000 to 70,000 ions collected), MS^2 Absolute Threshold (ranges from 5,000 to 50,000 ions selected for MS^2), and the number of MS^2 Precursor Ions (ranges from 2-6 ions). All of these parameters affect the quality of the MS results, including the Total Ion Chromatogram (TIC), which is a spectrum of all the MS-detected compounds prior to MS^2 fragmentation, as well as the total number of protein identifications (IDs) after searching the MS^2 *m/z* lists. Thus one aim was to test whether optimization of the aforementioned HPLC-ESI-Ion trap MS parameters would increase the number of TIC compounds detected, as well as the total number of protein IDs.

The same desalted, soluble protein trypsin digest from equally-mixed ^{14}N-high- and ^{15}N-optimal light *Synechococcus* 7002 cells was repeatedly injected into the HPLC-ESI-ion trap mass spectrometer to test the different instrument parameters. Results of the different optimization runs were compared with respect to: 1) Number of compounds in

the Total Ion Chromatogram (TIC), and 2) Number of protein IDs (from searches of the MS^2 mass lists in the MASCOT *Synechococcus* 7002-Genbank N14-15 + decoy database). HPLC programs characterized by a slower, mid-point (~50 min into the program) flow rate of 2 µl/min resulted in 699 total compounds and 25 protein IDs, as compared to only 417 compounds and 10 protein IDs for HPLC programs with constant flow rates of 5 or 10 µl/min (Table 1). A lower ion trap target of 20000 or 30000, and a Threshold Abs of 10000 or 20000 also contributed to increased TIC compounds and protein IDs (Table 1). Optimizing the number of MS^2 Precursor Ions from 4 to 6 resulted in a slight increase in TIC compounds (784 to 837) (Table 1). The optimized parameters resulted in higher MASCOT protein scores, with the highest MOWSE score of 995 vs 424 for the same protein, phycocyanin, alpha subunit (Table 2). The Matrix Science MASCOT MOWSE protein scores are derived from ion scores as a non-probabilistic basis for ranking protein hits, where individual ion scores >32 indicate identity or extensive homology ($p < 0.05$).

Table 1. HPLC-ESI-Ion trap MS/MS (MS^2) Parameter Optimizations for Total Ion Chromatogram (TIC) Compounds and Protein Identifications (IDs)

	Instrument Parameter	**Optimization**		**Total TIC Compounds**		**Total Protein IDs**	
		Pre	Post	Pre	Post	Pre	Post
HPLC	HPLC program flow rate	Constant 5 or 10 µl/min	Slower mid-program flow of 2 µl/min	417	699	10	25
Ion Trap MS	Trap Target (number of ions collected)	50,000-70,000	20,000-30,000	699	784	25	28
Ion Trap MS^2	Absolute Threshold (ions selected for AutoMS ^{2})	50,000	10,000-20,000	699	784	25	28
	Number of Precursor Ions (selected for AutoMS ^{2})	4	6	784	837	28	28

Table 2. Comparison of Protein Identifications from Optimizations of HPLC-ESI-Ion trap MS/MS (MS^2) Parameters

Ion trap MS^2 mass lists → MASCOT database Search → Protein IDs Repeated injection of same sample: soluble protein trypsin digest			
1st injection: **Pre-Optimization** (417 total compounds) **Protein hits**	Score*	Final injection: **Post-Optimization** (837 total compounds) **Protein hits**	Score
phycocyanin, alpha subunit	424	phycocyanin, alpha subunit	995
phycocyanin, beta subunit	365	allophycocyanin, beta subunit	982
allophycocyanin, beta subunit	300	phycocyanin, beta subunit	858
phycocyanin-associated, rod-terminating linker protein CpcD	173	phycocyanin-associated, rod-terminating linker protein CpcD	297
chaperonin, 60-kDa protein	129	allophycocyanin, alpha subunit	255
chaperonin, 10-kDa protein	86	chaperonin, 60-kDa protein	229
phycocyanin-associated, rod-linker protein	72	translation elongation factor Tu	199
Mn-superoxide dismutase	44	phycocyanin-associated rod-linker protein	147
ribulose-1,5-bisphosphate carboxylase, large subunit	43	chaperonin, 10-kDa protein	146
ATP synthase F1, alpha subunit	43	Ribulose bisphosphate carboxylase, small subunit	135
		photosystem I, subunit II	118
		ribulose-1,5-bisphosphate carboxylase, large subunit	105
		Photosystem II 12 kDa extrinsic protein (PsbU)	102
		ATP synthase beta chain	93
		Phycobilisome rod-core linker polypeptide cpcG (L-RC 28.5)	90
		allophycocyanin-associated phycobilisome 7.8-kDa core-linker polypeptide	81
		ribosome recycling factor	79
		allophycocyanin B alpha subunit	68
		conserved hypothetical protein	63
		Bacterial fructose-1,6-bisphosphatase, glpX-encoded superfamily	59
		trypsin precursor	53
		CP12 domain protein	52
		ribosomal protein S18	49
		DNA-binding protein HU	48
		chaperonin GroEL-II (Cpn 60)	43
		ATP synthase F1, alpha subunit	39
		RNA-binding protein	35
		2-phosphopyruvate hydratase (enolase)	32
Total Protein IDs:	**10**		**28**

*According to Matrix Science's MASCOT scoring: Protein scores are derived from ions scores as a non-probabilistic basis for ranking protein hits. Individual ions scores > 32 indicate identity or extensive homology ($p<0.05$). Ions score is -10*Log(P), where P is the probability that the observed match is a random event.

Sample Fractionation into SDS-PAGE Gel Bands Resulted in Additional Unique Protein Identifications

Since mass spectrometers tend to identify the most abundant peptides in a sample, it was important to investigate whether further separation of my ^{15}N-optimal- and ^{14}N-high-light mixed protein samples into SDS-PAGE gel-bands would increase the number of protein identifications (IDs).

Well-resolved SDS-PAGE of the membrane and soluble protein fractions were obtained and gel lanes cut into six and seven gel bands, respectively (Figure 1). These gel slices were digested with trypsin and processed for ESI-Ion trap MS as described in Methods.

The separate gel-band trypsin digests resulted in a similar number of soluble protein IDs as the bulk digest (29 vs 28) following ESI-Ion trap MS analyses. However, the gel-band analyses resulted in 19 additional unique protein IDs, with only 10 IDs shared between the bulk protein analysis & the separate gel-band analyses (Table 3). For the membrane protein fraction, the separate gel-band MS analyses resulted in 39 additional unique protein IDs (only 4 IDs shared with the bulk soluble protein analysis). Unfortunately, a bulk membrane protein digest was not tested for comparison because of problematic, electrospray ion trap performance. Testing the separate gel-band digests was given priority.

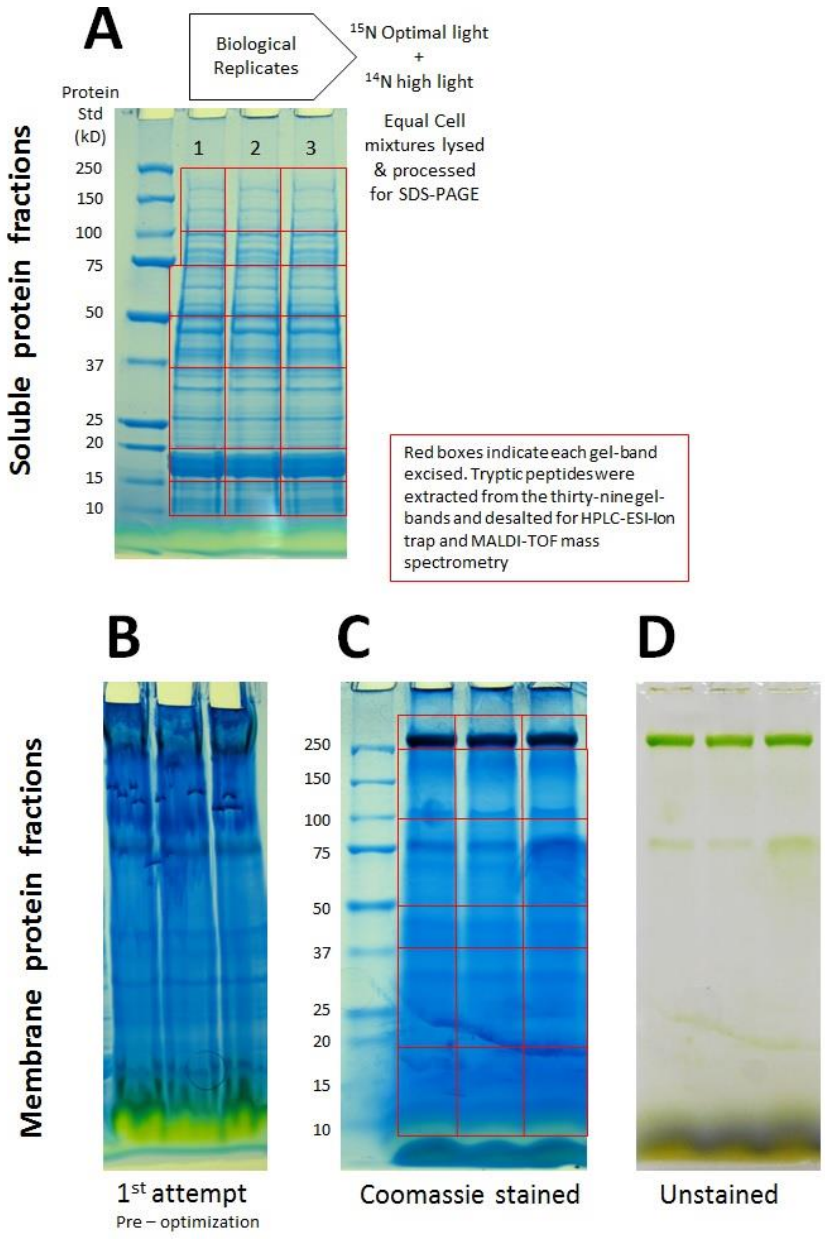

Figure 1. *Synechococcus* 7002 ^{15}N-Optimal- and ^{14}N-High-light mixed protein samples separated by SDS-PAGE. Cyanobacteria contain internal photosynthetic membranes, resulting in separate membrane (mp) and soluble (sp) protein fractions. Pre-cast SDS-PAGE gels (ThermoScientific Precise™, 4-20% acrylamide, 10-well) and a BioRad mini electrophoresis system were used to resolve these mp & sp fractions. 250 µg of each protein sample was overloaded per gel lane, to maximize the downstream trypsin-derived peptides for MS. Gels were stained with freshly prepared, MS-compatible "blue silver" Coomassie. **A)** Biological replicates of the sp gel lanes were cut into seven gel bands (10-15, 15-20, 20-37, 37-50, 50-75, 75-100, & 100-250 kD). **B-D)** The mp gel lanes were cut into six gel bands (<20, 20-37, 37-55, 55-100, 100-250, & ≥250 kD). The mp SDS-PAGE required optimization for improved resolution including resuspension in 4% SDS sample loading buffer (compared to 2% SDS), high-speed centrifugation of samples prior to loading, and slow electrophoresis (overnight at 10V compared to 1 h at 110-120V). The unstained gel showed distinct, green high molecular weight bands from intact photosystem protein complexes containing chlorophyll.

Table 3. Soluble and Membrane Protein Identifications (IDs) from separate SDS-PAGE gel-slices

SDS-PAGE separation by size → trypsin digests of gel-slices → HPLC-ESI-ion trap MS analysis → MASCOT database search of mass lists → Protein IDs

Soluble Protein IDs			
		Mass	Score
75-100 kD	glutamine synthetase type III	79251	274
	chaperone protein DnaK	68672	142
	phycobilisome core-membrane linker phycobiliprotein ApcE	99211	81
	putative sulfite reductase	87053	46
	translation elongation factor G	76566	41
50-75 kD	ATP synthase beta chain	52189	86
	ribulose-1,5-bisphosphate carboxylase, large subunit	52225	72
37-50 kD	translation elongation factor Tu	44525	472
	fructose-bisphosphate aldolase, class II, Calvin cycle subtype	38598	214
	bacterial fructose-1,6-bisphosphatase, glpX-encoded superfamily	37313	196
	IMP dehydrogenase family protein	40087	88
	iron transport protein	39189	70
	phosphoribulokinase	37655	68
	ferredoxin-NADP reductase	44986	63
	geranylgeranyl reductase	44909	60
	resolvase	11778	34
	tryptophan synthase, beta subunit	45115	32
20-37 kD	phycocyanin-associated rod linker protein	32253	260
	phycobilisome rod-core linker polypeptide cpcG (L-RC 28.5)	28493	122
	photosystem II D1 subunit PsbA-II (Qb protein)	38442	58
15-20 kD	phycocyanin, alpha subunit	17611	981
	allophycocyanin alpha subunit	17275	315
	allophycocyanin, beta subunit	17211	291
	phycocyanin, beta subunit	18324	135
10-15 kD	phycocyanin, alpha subunit	17611	120
	ribulose bisphosphate carboxylase, small subunit	13204	113
	nitrogen regulatory protein P-II	12425	105
	carbon dioxide concentrating mechanism protein	11138	70
	ribosomal protein L7/L12	13368	45
	cytochrome c-550 precursor (Cytochrome c550) (Low potential cytochrome c550)	18766	43
Total: 29			
Total unique IDs: 19			

Membrane Protein IDs			
		Mass	Score
≥ 250 kD	photosystem I protein A2	81585	437
	conserved hypothetical protein	65875	218
	photosystem I subunit II	15586	194
	photosystem I reaction center subunit XI	15608	159
	photosystem I P700 chlorophyll A apoprotein A1	81336	127
	phycobilisome core-membrane linker phycobiliprotein ApcE	99211	123
	S-layer like protein; probable porin	60256	84
	conserved hypothetical protein	57860	81
100-250 kD	phycobilisome core-membrane linker phycobiliprotein ApcE	99211	534
	S-layer like protein; probable porin	60256	388
	conserved hypothetical protein	65875	252
	conserved hypothetical protein	57860	103
	photosystem I protein A2	81585	98
	glutamine synthetase type III	79251	69
	short-chain dehydrogenase/reductase family enzyme	45484	38
	glutaredoxin		34
	imidazoleglycerol phosphate synthase, cyclase subunit		34
50-100 kD	glutamine synthetase type III	79251	165
	photosystem I protein A2	81585	157
	phycobilisome core-membrane linker phycobiliprotein ApcE	99211	118
	photosystem I P700 chlorophyll A apoprotein A1	81336	111
	photosystem I subunit II	15586	45
	ATP-dependent metalloprotease FtsH subfamily	67517	40
	uncharacterized protein involved in exopolysaccharide biosynthesis	83803	38
	ATP-dependent metalloprotease, FtsH family	68528	38
	D-3-phosphoglycerate dehydrogenase	55928	37
37-50 kD	photosystem II protein	55764	751
	photosystem II 44 kDa subunit reaction center protein	51516	323
	phosphoglycerate kinase	41528	112
	ribulose-1,5-bisphosphate carboxylase, large subunit	52225	88
	iron transport protein	39189	81
	photosystem I subunit II	15586	78
	carbon dioxide concentrating mechanism protein	70026	69
	glutamine synthetase type III	79251	59
	geranylgeranyl reductase	44909	57
	ABC transporter, branched-chain amino acid transport, periplasmic binding protein	47738	50
	photosystem I protein A2	81585	42
	ATP synthase F1, alpha subunit	54092	37
	protein-export membrane protein SecD	49346	35
	phycobilisome core-membrane linker phycobiliprotein ApcE	99211	33
20-37 kD	phycocyanin-associated rod linker protein	32253	334
	photosystem II D1 subunit PsbA-II	38442	131
	photosystem q(b) protein	39592	131
	light-dependent protochlorophyllide reductase	35346	81
	photosystem II manganese stabilizing protein PsbO	30322	77
	photosystem I protein A2	81585	70
	apocytochrome f precursor	34853	70
	conserved hypothetical protein	32243	67
	ribosomal protein L1	26017	61
	NADH dehydrogenase subunit K	27089	61
	photosystem II D2 protein	39574	54
	NADH dehydrogenase subunit A	40491	52
	ribosomal protein S3	27171	46
	heptosyltransferase family protein	34836	35
≤ 20 kD	photosystem I reaction center subunit XI	15608	89
	phycocyanin-associated rod linker protein	32253	51
	photosystem II D1 subunit PsbA-II (Qb protein)	38442	48
	cytochrome b6	25162	46
	photosystem I subunit II	15586	46
	photosystem I reaction center subunit III, PsaF	18310	42
	phycobilisome rod-core linker polypeptide cpcG	28493	37
	conserved hypothetical protein	16928	36
Total: 62			
Total unique IDs: 43			

* Highlighted proteins were also IDed via MS analysis of the bulk soluble protein digest

^{15}N-Metabolic Labeling of *Synechococcus* 7002 Cellular Proteins/Tryptic Peptides

^{15}N-Metabolic labeling of *Synechococcus* 7002 cells for metabolite profiling by mass spectrometry has been previously demonstrated [14], but not for proteomic analyses. Furthermore, ^{15}N metabolic labeling of the cyanobacterium *Euhalothece* sp. BAA001 has been shown to be an excellent approach for MS-based quantification of protein responses to different culture growth conditions [13]. Thus it was important to test the ^{15}N-metabolic labeling approach for detecting *Synechococcus* 7002 tryptic peptides from different culture conditions (high- versus optimal-light) by mass spectrometry. The soluble protein fraction from a *Synechococcus* 7002 ^{14}N-high- and ^{15}N-optimal-light cell mixture was analyzed via both ESI-Ion trap and MALDI-TOF mass spectrometry.

Both ^{14}N-high- and ^{15}N-optimal-light peptides were detected via ESI-Ion trap and MALDI-TOF MS analyses (Figure 2). Matching ^{14}N/^{15}N peptide pairs were mass/charge (*m/z*) shifted due to the ^{14}N versus ^{15}N-incorporation. Mass shifts were equal to the number of nitrogens in the amino acid sequence divided by the peptide ion charge, and can be defined in atomic mass units (amu or u) where 1 amu approximates the mass of one nucleon (Figure 2A-B). The similar peak patterns between the ^{14}N/^{15}N peak envelopes suggests nearly complete ^{15}N incorporation, since incomplete ^{15}N-labeling could alter the heavy peptide envelope pattern (Figure 2B). Finally, the tandem MS/MS (MS^2) collision-induced (CID) fragmentation spectra are similar as expected between

matching ^{14}N and ^{15}N peptide pairs, since they share the same amino acid chemistry and corresponding response to CID peptide fragmentation (Figure 2C).

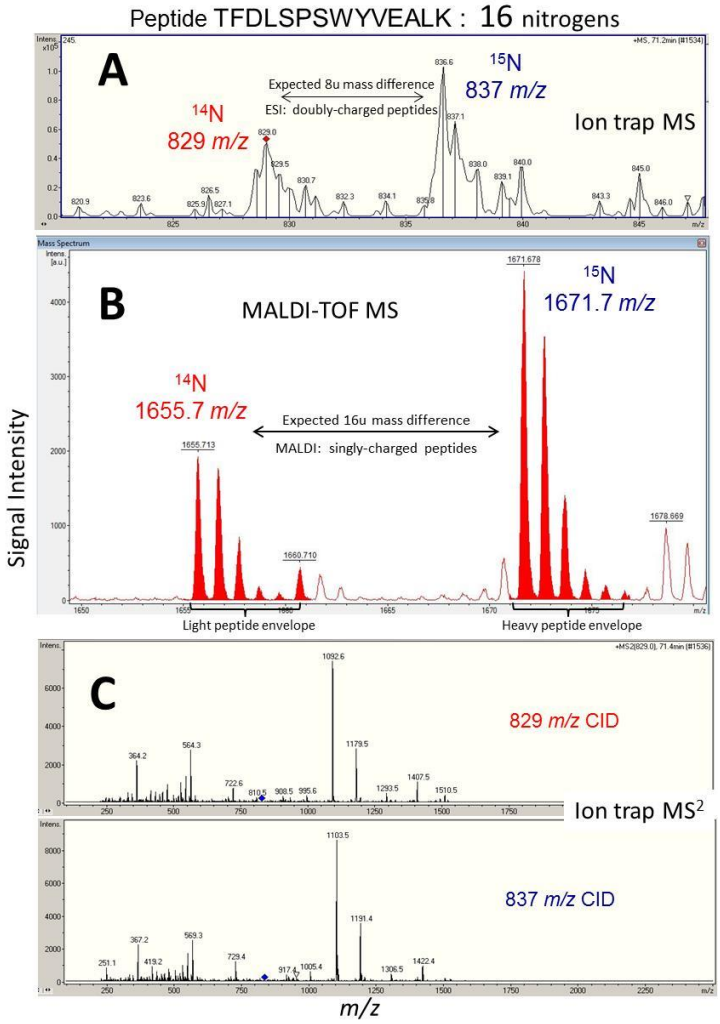

Figure 2. Example of peptide mass shifts resulting from ^{14}N versus ^{15}N incorporation. The peptide TFDLSPSWYVEALK, containing 16 nitrogens, originates from *Synechococcus* 7002 phycocyanin, alpha subunit protein. The ^{14}N peptide is from a culture grown under 2h high light exposure, and the ^{15}N variant is from a culture grown under optimal light. Panels A and C are mass spectra (MS and MS^2, respectively) from a Bruker Esquire™ 3000*plus* electrospray ion trap instrument, and Panel B is the mass spectrum from a Bruker Reflex IV MALDI-TOF instrument. The MALDI-TOF MS has improved peak resolution as compared to the ion trap MS, and clearly shows a higher relative signal intensity of the peptide from the ^{15}N optimal light culture. The ion trap provides CID-fragmentation MS^2 spectra for both the ^{14}N (829 *m/z*) and ^{15}N (837 *m/z*) peptides, whose fragmentation masses were database-searched to identify the peptide amino acid sequences. **Panel A**: The heavy ^{15}N 837 *m/z* peptide is shifted from the ^{14}N 829 *m/z* peptide by the expected isotopic 8 amu, which corresponds to the number of nitrogens in the amino acid sequence divided by the ion charge (16 nitrogens divided by the ion charge of 2+). **Panel B**: The ^{15}N 1671.7 *m/z* peptide is shifted from the ^{14}N 1655.7 *m/z* peptide is shifted from the by the expected isotopic 16 amu (16 nitrogens divided by the ion charge of 1+). MALDI ionization tends to result in singly-charged peptide ions. **Panel C:** The MS^2 spectra of both the ^{14}N and ^{15}N peptides have similar fragmentation patterns (masses), suggesting that the light and heavy forms of the peptide fragment similarly within the ion trap, regardless of the isotopic nitrogen incorporation. The individual *m/z* peak values are isotopically shifted between the two spectra, due to their separate ^{14}N/^{15}N incorporation. The small blue diamonds indicate the precursor peptide ions, whose signals are negligible after complete CID-fragmentation within the ion trap.

Identification of Predominant Soluble and Membrane Proteins by Cross-Referencing of MALDI-TOF and ESI-Ion Trap Mass Spectrometry Data

Although the CID fragmentation function of the ESI-Ion trap instrument provided crucial MS/MS (MS^2) mass lists required for MASCOT searches and peptide amino acid sequences for protein identification—the instrument's inconsistent performance, particularly with its electrospray ionization, limited the data collection from the gel slices to a single replicate of these samples. In contrast, the MALDI-TOF instrument functioned robustly, and excellent peptide spectra of all three biological replicates and from 13 gel-slices were obtained (39 total samples analyzed).

In general, the MALDI-TOF mass spectrometer had superior reproducibility, peak resolution, and mass accuracy than the ESI-Ion trap. These characteristics, plus the more user-friendly analysis software and the ability to compare all three biological replicates (allowing for statistical analyses), made the MALDI-TOF preferable for the $^{14}N/^{15}N$ peptide quantification comparisons. However, since the UW-Oshkosh Bruker Reflex IV MALDI-TOF instrument lacks the CID/MS^2 capability for peptide sequencing, the MALDI-TOF peptides could only be identified by cross-referencing the parent peptide ions of known masses to the single-replicate ESI-Ion trap mass lists obtained by MS^2 peptide fragmentation.

Cross-matched peptides—sequenced via ESI-ion trap MS^2 data, and also detected (based on the parent peptide masses) via MALDI-TOF MS—were generally doubly- and singly-charged, respectively, reflecting the characteristic peptide ionization patterns of

those instruments. For the soluble protein fraction, 12 peptides specific to 7 proteins were cross-detected (Table 4). For the membrane protein fraction, 13 peptides specific to 7 proteins were cross-detected (Table 5). Abundant, soluble-fraction phycobilisome light harvesting proteins and membrane-fraction photosystem proteins were the predominant cross-detected proteins. Only three non-photosynthetic proteins were detected in these comparisons. These were translation elongation factor Tu, glutamine synthetase type III, and S-layer like protein, a probable porin.

The MALDI-TOF spectra occasionally showed that one or both of an $^{14}N/^{15}N$ peptide pair were occluded by the spectral envelope of a different peptide of similar mass. Unfortunately, if a peptide signal was occluded in this way, the signal intensity could not be used for $^{14}N/^{15}N$ relative peptide/protein quantity comparisons, because the occluding peptide contributed to the overall signal intensity.

Table 4. Soluble Peptides/Proteins Identified by ESI-Ion trap MS^2 and Cross-detected by MALDI-TOF MS

Soluble Protein Identifications (IDs)							
gel slice	**No. of MALDI-TOF Cross-IDs[1]**	ESI-Ion trap MS^2 sequenced reference IDs	Score[2]	**gel slice**	**No. of MALDI-TOF Cross-IDs**	ESI-Ion trap MS^2 sequenced reference IDs	Score
75-100 kD	**2 peptides**	**glutamine synthetase type III** **R.VQAIQQITNR.T** **K.VLVQGEPDGSSFPNGGIR.D**	274	**20-37 kD**	**3 peptides**	**phycocyanin-associated rod linker protein** **K.FLYNNFQTR.V** **R.LGTAAFDQSPVELR.A** **R.NTTSAVVGPSGVNEGWAFR.S**	260
		chaperone protein DnaK	142		**2 peptides**	**phycobilisome rod-core linker polypeptide cpcG (L-RC 28.5)** **R.VSAADISLAAVPYRN.-** **M.TIPLLQYAPSSQNTR.V**	122
		phycobilisome core-membrane linker phycobiliprotein ApcE	81				
		putative sulfite reductase	46				
		translation elongation factor G	41				
50-75 kD		ATP synthase beta chain	86			photosystem II D1 subunit PsbA-II (Qb protein)	58
	1 peptide	**ribulose-1,5-bisphosphate carboxylase, large subunit** **R.FPVALIK.T**	72	**15-20 kD**	**2 peptides**	**phycocyanin, alpha subunit** **K.TPLTEAVALADSQGR.F** **R.FLSNTELQYLYGR.L**	981
37-50 kD	**1 peptide**	**translation elongation factor Tu** **K.TLDEGMAGDNVGVLLR.G**	472		**1 peptide**	**allophycocyanin alpha subunit** **K.SLGTPVDAVAQAVR.E**	315
		fructose-bisphosphate aldolase, class II, Calvin cycle subtype	214			allophycocyanin, beta subunit	291
		bacterial fructose-1,6-bisphosphatase, glpX-encoded superfamily	196			phycocyanin, beta subunit	135
		IMP dehydrogenase family protein	88				
		iron transport protein	70	**10-15 kD**	**No MALDI-TOF Cross IDs**	phycocyanin, alpha subunit	120
		phosphoribulokinase	68			ribulose bisphosphate carboxylase, small subunit	113
		ferredoxin-NADP reductase	63			nitrogen regulatory protein P-II	105
		geranylgeranyl reductase	60			carbon dioxide concentrating mechanism protein	70
		resolvase	34			ribosomal protein L7/L12	45
		tryptophan synthase, beta subunit	32			cytochrome c-550 precursor (Low potential cytochrome c550)	43
Total: 12 peptides for 7 proteins							

[1]Twelve peptides corresponding to seven proteins identified from ESI-Ion trap MS^2 data were cross-detected by MALDI-TOF MS and highlighted in pink/red. No peptides were cross-detected in the 10-15kD gel slice. [2]Scores shown are MOWSE protein scores based on the sum of individual peptide scores for each protein.

Table 5. Membrane Peptides/Proteins Identified by ESI-Ion trap MS^2 and Cross-detected by MALDI-TOF MS

Membrane Protein Identifications (IDs)							
gel slice	No. of MALDI-TOF Cross-IDs[1]	ESI-Ion trap MS^2 sequenced reference IDs	Score[2]	gel slice	No. of MALDI-TOF Cross-IDs	ESI-Ion trap MS^2 sequenced reference IDs	Score
≥ 250 kD	2 peptides	**photosystem I protein A2** **K.FSQDLAQDPTTR.R** **K.FSQDLAQDPTTR.RJ**	437	37-50 kD	1 peptide	**photosystem II protein** **R.AQLGEPFEFDTETLGSDGVFR.T**	751
		conserved hypothetical protein	218			reaction center protein	323
	2 peptides	**photosystem I subunit II** **K.FGGSTGGLLAAAEREEK.Y** **R.VFPSGETQFLYPLDGVPSEK.V**	194			phosphoglycerate kinase	112
		photosystem I reaction center subunit XI	159			ribulose-1,5-bisphosphate carboxylase, large subunit	88
	1 peptide	**photosystem I P700 chlorophyll A apoprotein A1** **R.LVPDKGQLGFR.F**	127			iron transport protein	81
		phycobilisome core-membrane linker phycobiliprotein ApcE	123			photosystem I subunit II	78
	1 peptide	**S-layer like protein; probable porin** **R.IAEDTTIDDVVFTPDFLR.D**	84			carbon dioxide concentrating mechanism protein	69
		conserved hypothetical protein	81			glutamine synthetase type III	59
100-250 kD	4 peptides	**phycobilisome core-membrane linker phycobiliprotein ApcE** **R.ALELAFR.H** **K.EFYTPYPNTK.V** **K.QFFEPFINSR.A** **R.FPTLPAANFPNTER.L**	534			geranylgeranyl reductase	57
		S-layer like protein; probable porin	388			ABC transporter, branched-chain amino acid transport, periplasmic binding protein	50
		conserved hypothetical protein	252			photosystem I protein A2	42
		conserved hypothetical protein	103			ATP synthase F1, alpha subunit	37
		photosystem I protein A2	98			protein-export membrane protein SecD	35
		glutamine synthetase type III	69			phycobilisome core-membrane linker phycobiliprotein ApcE	33
		short-chain dehydrogenase/reductase family enzyme	38	20-37 kD	1 peptide	**phycocyanin-associated rod linker protein** **K.FLYNNFQTR.V**	334
		glutaredoxin	34			photosystem II D1 subunit PsbA-II	131
		imidazoleglycerol phosphate synthase, cyclase subunit	34			photosystem q(b) protein	131
50-100 kD		glutamine synthetase type III	165			light-dependent protochlorophyllide reductase	81
		photosystem I protein A2	157			photosystem II manganese stabilizing protein PsbO	77
		phycobilisome core-membrane linker phycobiliprotein ApcE	118			photosystem I protein A2	70
	1 peptide	**photosystem I P700 chlorophyll A apoprotein A1** **R.LVPDKGQLGFR.F**	111			apocytochrome f precursor	70
		photosystem I subunit II	45			conserved hypothetical protein	67
		ATP-dependent metalloprotease FtsH subfamily	40			ribosomal protein L1	61
		uncharacterized protein involved in exopolysaccharide biosynthesis	38			NADH dehydrogenase subunit K	61
		ATP-dependent metalloprotease, FtsH family	38			photosystem II D2 protein	54
		D-3-phosphoglycerate dehydrogenase	37			NADH dehydrogenase subunit A	52
						ribosomal protein S3	46
						heptosyltransferase family protein	35
				≤ 20 kD	No MALDI-TOF Cross IDs	photosystem I reaction center subunit XI	89
						phycocyanin-associated rod linker protein	51
						photosystem II D1 subunit PsbA-II (Qb protein)	48
						cytochrome b6	46
						photosystem I subunit II	46
						photosystem I reaction center subunit III, PsaF	42
						phycobilisome rod-core linker polypeptide cpcG	37
						conserved hypothetical protein	36
Total: 13 peptides for 7 proteins							

[1]Thirteen peptides corresponding to seven proteins identified from ESI-Ion trap MS^2 data were cross-detected by MALDI-TOF MS and highlighted in pink/red. No peptides were cross-detected in the ≤ 20 kD gel slice. [2]Scores shown are MOWSE protein scores based on the sum of individual peptide scores for each protein.

Photosystem and Phycobilisome Relative Protein Levels Decreased Approximately 2-fold in *Synechococcus* 7002 Cells Grown Under High Light Intensity

For the high-light culture growth conditions tested, 2 h exposure to 2000 µmol photons m^{-2} s^{-1} high-light prior to culture harvest as opposed to continuous optimal light exposure of 200 µmol photons m^{-2} s^{-1}, it was important to determine whether the MALDI-TOF MS cross-detected *Synechococcus* 7002 protein levels were significantly altered.

Quantitative peak area comparisons and paired t-tests were performed for the ^{14}N-high- and ^{15}N-optimal-light MALDI-TOF MS peptides that were cross-identified from ESI-Ion trap MS^2 data. Photosystem I proteins A2, subunit II, and P700 chlorophyll A apoprotein A1 levels declined by 68.5%, 68.2%, and 63.1%, respectively (with *p* values of 0.021, 0.0097, and 0.023) in the high-light relative to optimal-light cultures (Figures 3-4). However, the same peptide, R.LVPDKGQLGFR.F for PSI P700 chlorophyll A apoprotein A1, showed no significant change in high light when detected in a different membrane protein gel slice (55-100 kD instead of 250+ kD, $p = 0.39$, Figure 4). Although not statistically significant (at $p < 0.05$), photosystem II showed a 46% decrease in high light cultures ($p = 0.08$) (Figure 5).

Allophycocyanin and phycocyanin alpha subunits of the phycobilisome light-harvesting complex, declined by 52.1% and 38.5% (*p* values 0.118 and 0.092) in the high-light relative to optimal-light cultures (Figure 6). In the soluble protein (sp) and membrane protein (mp) 20-37 kD gel slices, the peptide K.FLYNNFQTR.V for

phycocyanin-associated rod linker protein showed an average of 43.2% decrease (*p* 0.031) in high-light relative to optimal-light cultures (Figure 7). Two other peptides for phycocyanin-associated rod linker protein showed an average decline of 67.2% (*p* 0.33, Figure 7) in the high-light cultures.

The remaining MALDI-TOF MS cross-detected phycobilisome proteins were rod-core linker cpcG and core-membrane linker ApcE, which showed average decreases 50.1% and 52.7% (*p* 0.042 and 0.015) in the high-light cultures (Figures 8-9). An exception was the small peptide R.ALELAFR.H for phycobilisome core-membrane linker ApcE, which had a non-significant +77.1% percent (p 0.075, Figure 9) change in high-light. The final photosynthesis/carbon-fixation-related protein detected was the large subunit of ribulose-1,5-bisphosphate carboxylase. Only detected in one biological replicate (n =1), where it showed an insignificant +19.4% change in high-light (Figure 10).

Finally, the three non-photosynthesis related proteins that were cross-detected from the MALDI-TOF MS and ESI-Ion trap MS^2 data were glutamine synthetase type III, translation elongation factor Tu, and S-layer like protein. All three showed no significant differences in high-light relative to optimal-light cultures (Figures 11-12).

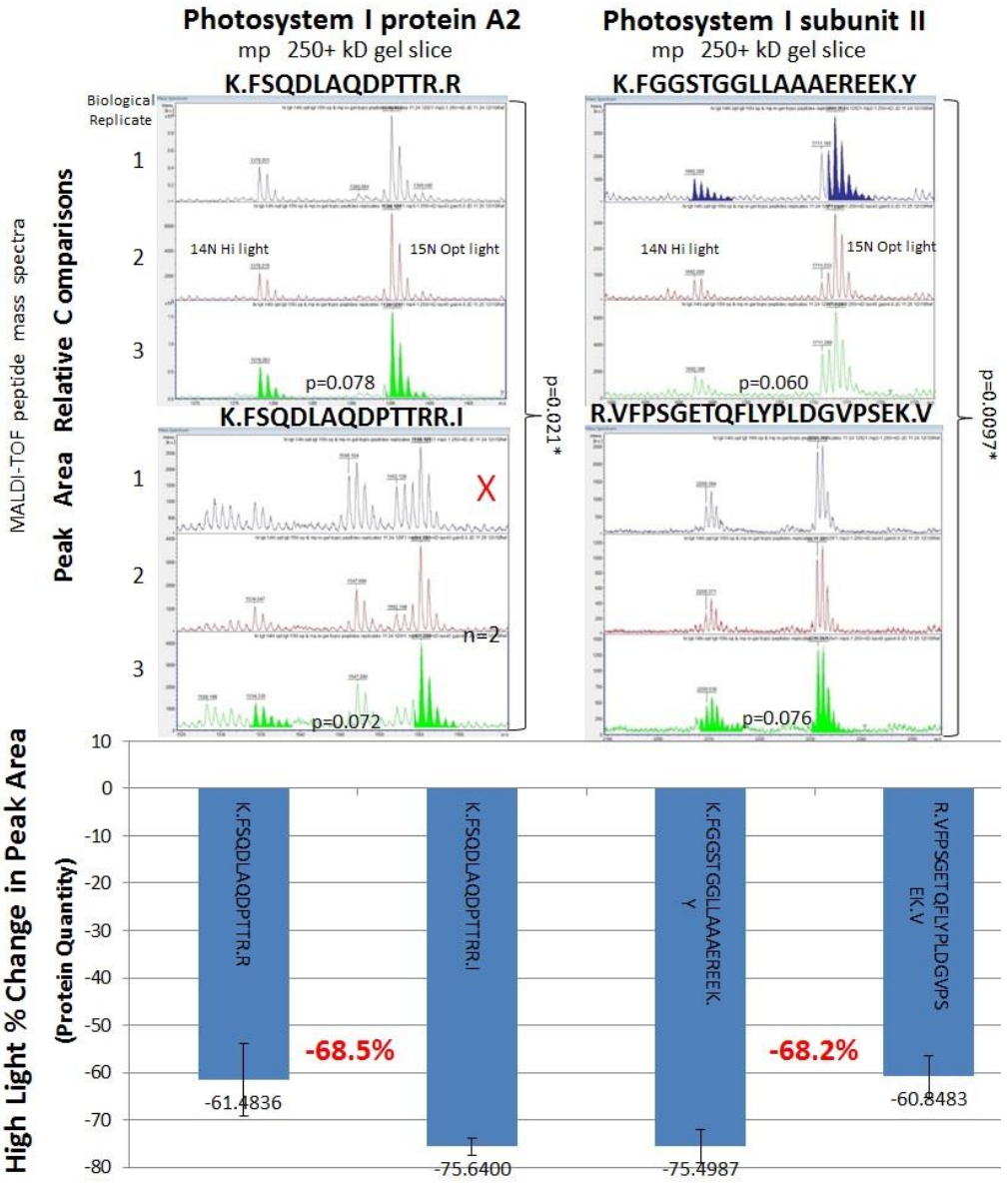

Figure 3. Photosystem I protein A2 and subunit II quantitative light- and heavy-peptide peak area comparisons from MALDI-TOF MS spectra. Peptides that were detected and analyzed were cross-identified from ESI-Ion trap MS^2 data. Spectra are shown for each peptide from all three biological replicates sampled. Red "X" indicates a biological replicate with poor peak resolution that was excluded from the statistical analyses. All t-tests are paired, and the vertical t-tests include both peptides (and replicates) for the same protein. The bar graph shows percent changes in peptide and corresponding protein levels in samples from high-light relative to optimal light cultures from the three biological replicates. Because matched peptides from both culture conditions (^{14}N high- vs ^{15}N optimal-light) were compared, the changes in peak area signal intensities provide relative protein quantification. The percent changes in red are the average of the two peptide data for the given protein. mp refers to the membrane protein fraction.

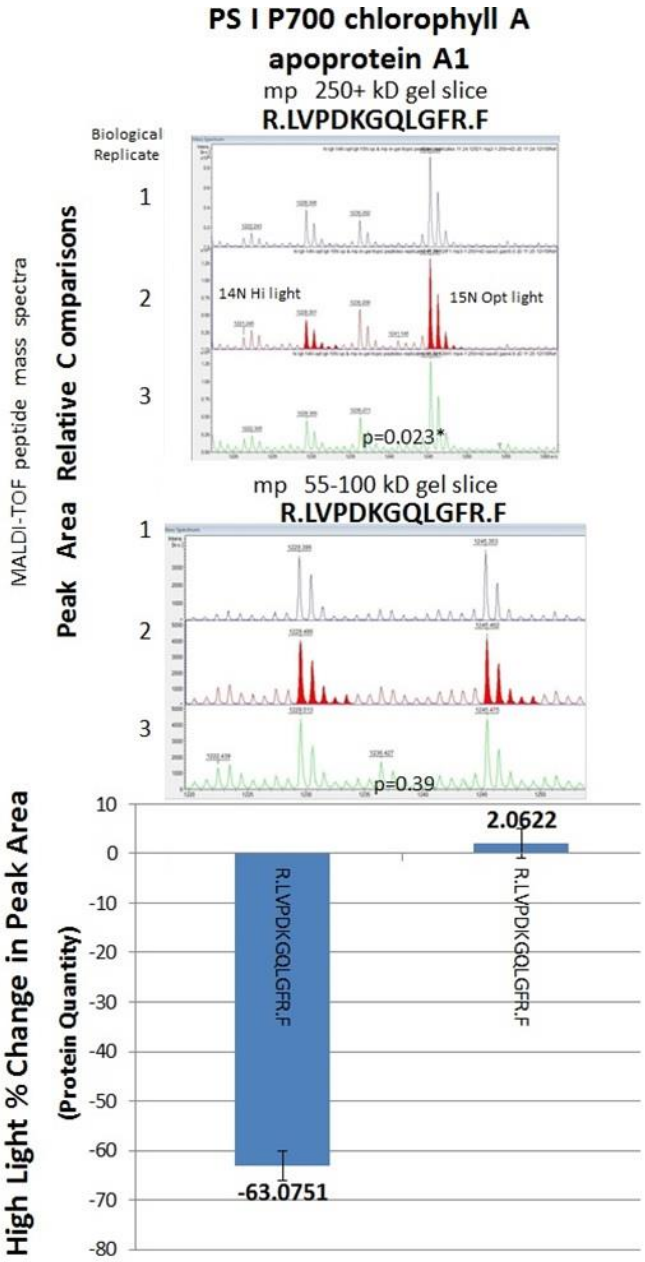

Figure 4. Photosystem (PS) I P700 chlorophyll A apoprotein A1 quantitative light- and heavy-peptide peak area comparisons from MALDI-TOF MS spectra. Peptides that were detected and analyzed were cross-identified from ESI-Ion trap MS^2 data. The same peptide R.LVPDKGQLGFR.F was detected into two different gel slices, 250+ kD and 55-100 kD. The 250+ kD gel slice may represent the peptide in relation to the intact PS I complex. Spectra are shown for each peptide from all three biological replicates sampled. All t-tests are paired. The bar graph shows percent changes in peptide levels in samples from high-light relative to optimal light cultures from the three biological replicates. Because matched peptides from both culture conditions (^{14}N high- vs ^{15}N optimal-light) were compared, the changes in peak area signal intensities may provide relative protein quantification. mp refers to the membrane protein fraction.

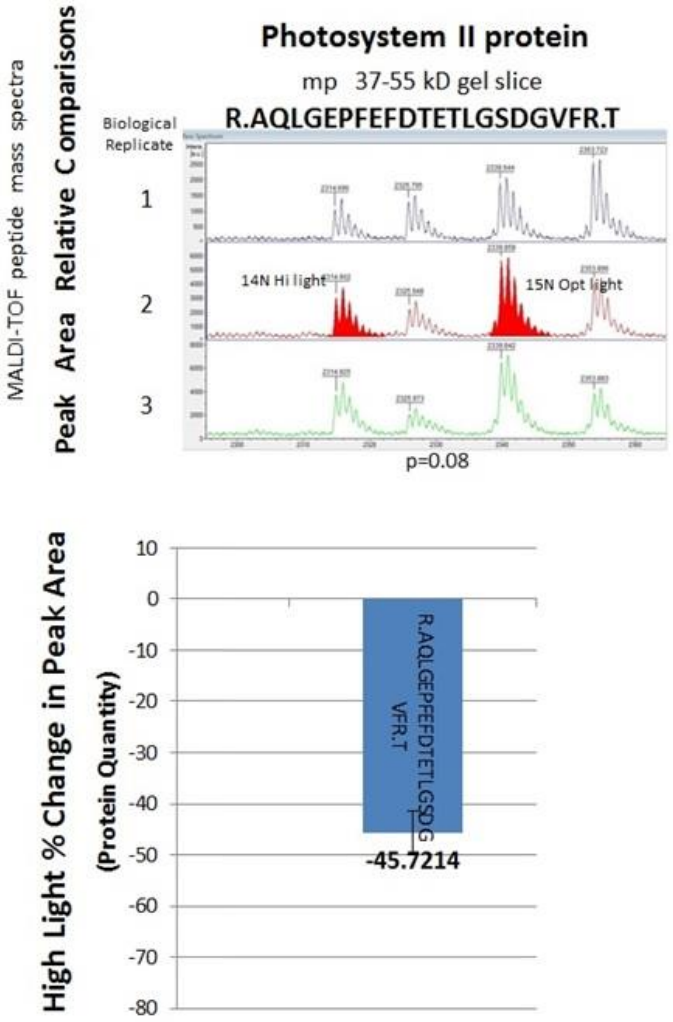

Figure 5. Photosystem II protein quantitative light- and heavy-peptide peak area comparisons from MALDI-TOF MS spectra. Peptides that were detected and analyzed were cross-identified from ESI-Ion trap MS^2 data. Spectra are shown for each peptide from all three biological replicates sampled. T-test is paired. The bar graph shows the average percent change in peptide levels in samples from high-light relative to optimal light cultures from the three biological replicates. Because matched peptides from both culture conditions (^{14}N high- vs ^{15}N optimal-light) were compared, the changes in peak area signal intensities may provide relative protein quantification. mp refers to the membrane protein fraction.

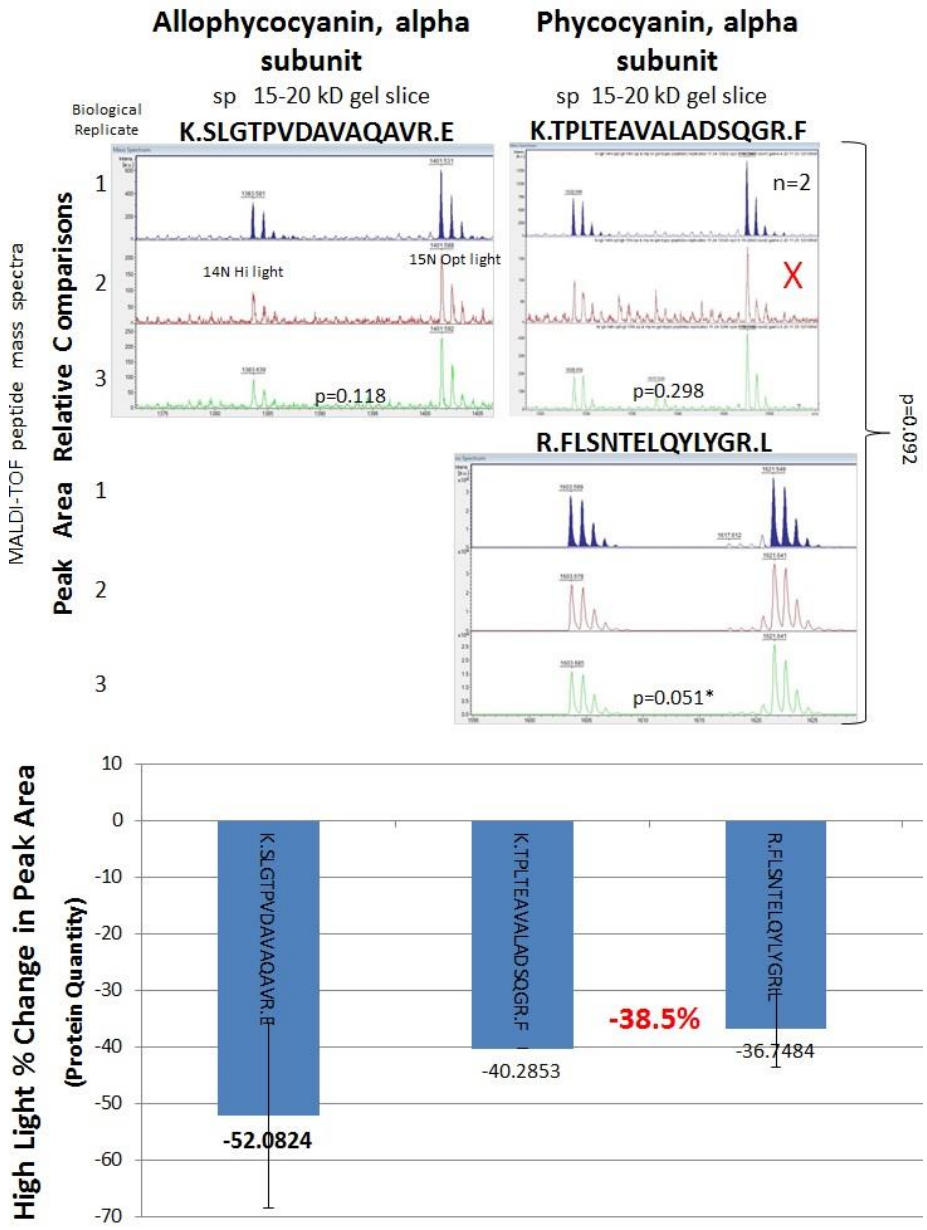

Figure 6. Allophycocyanin and Phycocyanin (alpha subunits) quantitative light- and heavy-peptide peak area comparisons from MALDI-TOF MS spectra. Peptides that were detected and analyzed were cross-identified from ESI-Ion trap MS^2 data. Spectra are shown for each peptide from all three biological replicates sampled. Red "X" indicates a biological replicate with poor peak resolution that was excluded from the statistical analyses. All t-tests are paired, and the vertical t-test includes both peptides (and replicates) for the same protein. The bar graph shows percent changes in peptide and corresponding protein levels in samples from high-light relative to optimal light cultures from the three biological replicates. Because matched peptides from both culture conditions (^{14}N high- vs ^{15}N optimal-light) were compared, the changes in peak area signal intensities provide relative protein quantification. The percent change in red is the average of the two peptide data for the given protein. sp refers to the soluble protein fraction.

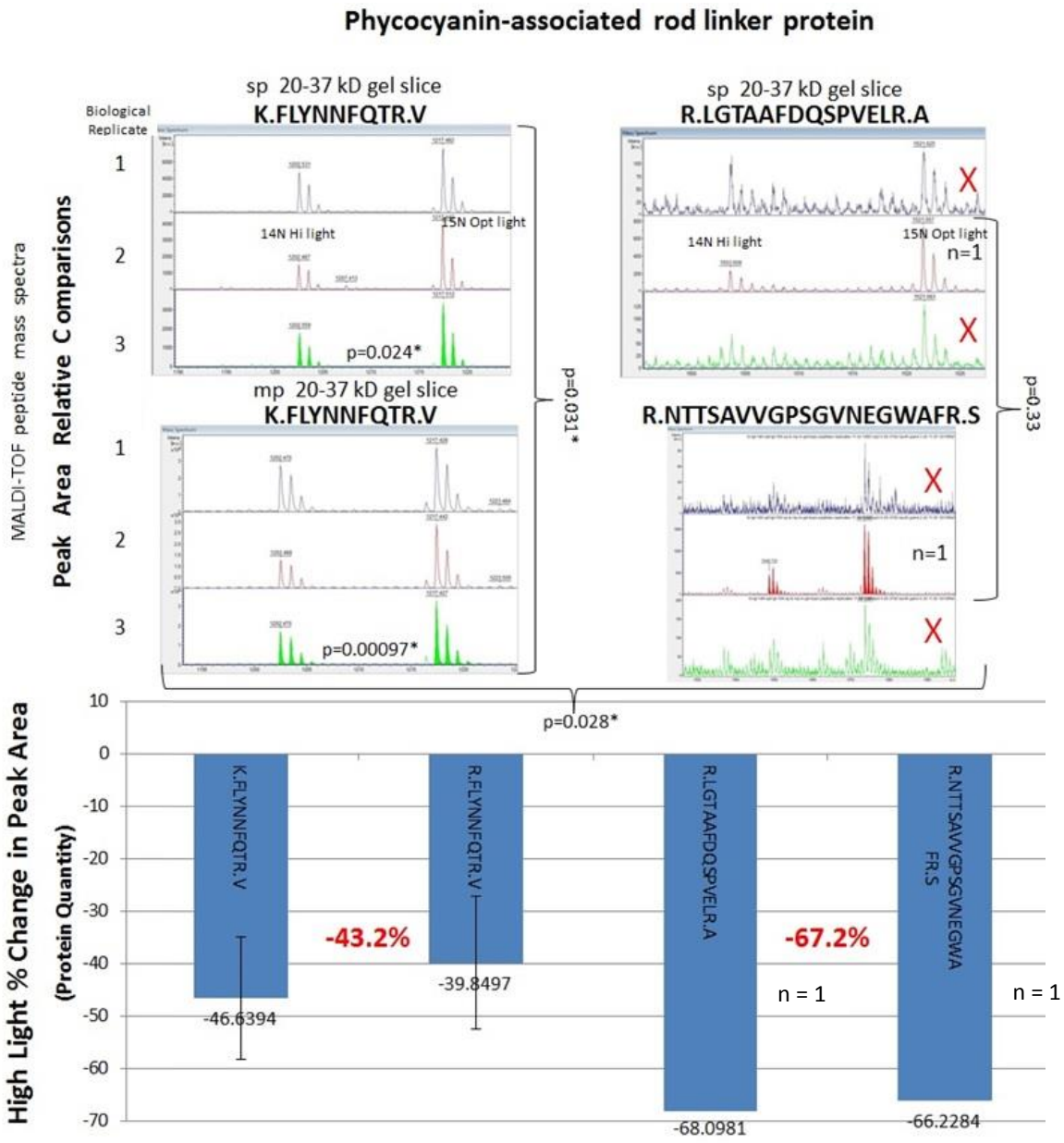

Figure 7. Phycocyanin-associated rod linker protein quantitative light- and heavy-peptide peak area comparisons from MALDI-TOF MS spectra. Peptides that were detected and analyzed were cross-identified from ESI-Ion trap MS^2 data. Spectra are shown for each peptide from all three biological replicates sampled. Red "X"s indicate biological replicates with poor peak resolution that were excluded from the statistical analyses. All t-tests are paired, and the vertical t-test includes both peptides (and replicates) for the same protein. The bar graph shows percent changes in peptide and corresponding protein levels in samples from high-light relative to optimal light cultures from the three biological replicates. Because matched peptides from both culture conditions (^{14}N high- vs ^{15}N optimal-light) were compared, the changes in peak area signal intensities provide relative protein quantification. The percent changes in red are the averages of the two peptide data for the given protein. sp and mp refer to the soluble and membrane protein fractions, respectively.

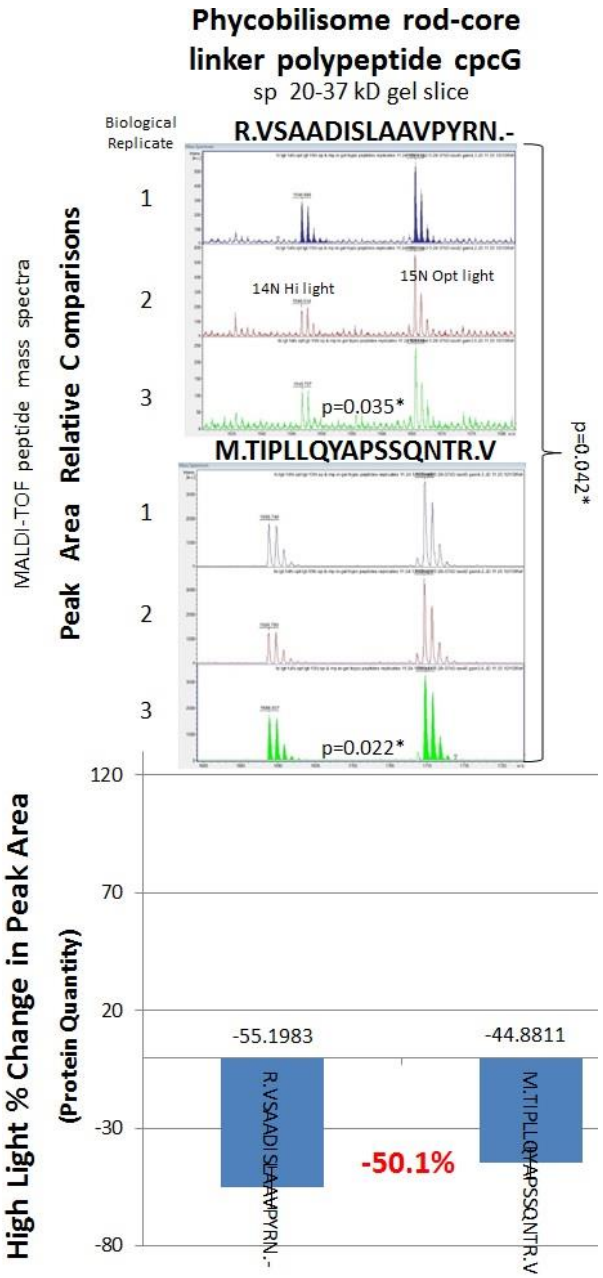

Figure 8. Phycobilisome rod-core linker polypeptide cpcG quantitative light- and heavy-peptide peak area comparisons from MALDI-TOF MS spectra. Peptides that were detected and analyzed were cross-identified from ESI-Ion trap MS^2 data. Spectra are shown for each peptide from all three biological replicates sampled. All t-tests are paired, and the vertical t-test includes both peptides (and replicates) for the same protein. The bar graph shows percent changes in peptide and corresponding protein levels in samples from high-light relative to optimal light cultures from the three biological replicates. Because matched peptides from both culture conditions (^{14}N high- vs ^{15}N optimal-light) were compared, the changes in peak area signal intensities provide relative protein quantification. The percent change in red is the average of the two peptide data for the given protein. sp refers to the soluble protein fraction.

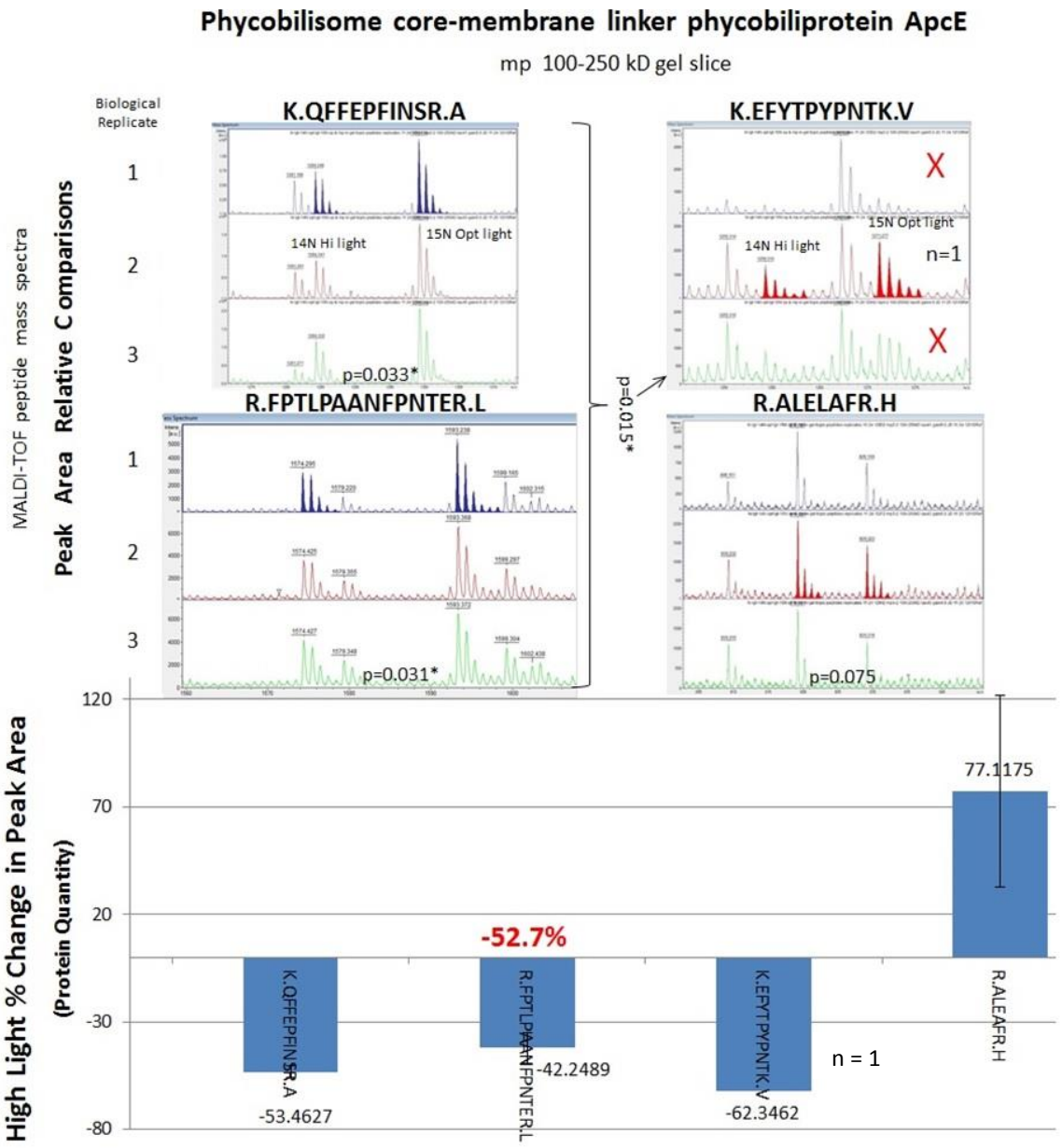

Figure 9. Phycobilisome core-membrane linker phycobiliprotein ApcE quantitative light- and heavy-peptide peak area comparisons from MALDI-TOF MS spectra. Peptides that were detected and analyzed were cross-identified from ESI-Ion trap MS^2 data. Spectra are shown for each peptide from all three biological replicates sampled. Red "X"s indicate biological replicates with poor peak resolution that were excluded from the statistical analyses. All t-tests are paired, and the vertical t-test includes three peptides (and replicates) for the same protein. The bar graph shows percent changes in peptide and corresponding protein levels in samples from high-light relative to optimal light cultures from the three biological replicates. Because matched peptides from both culture conditions (^{14}N high- vs ^{15}N optimal-light) were compared, the changes in peak area signal intensities provide relative protein quantification. The percent change in red is the average of the three peptide data for the given protein. mp refers to the membrane protein fraction.

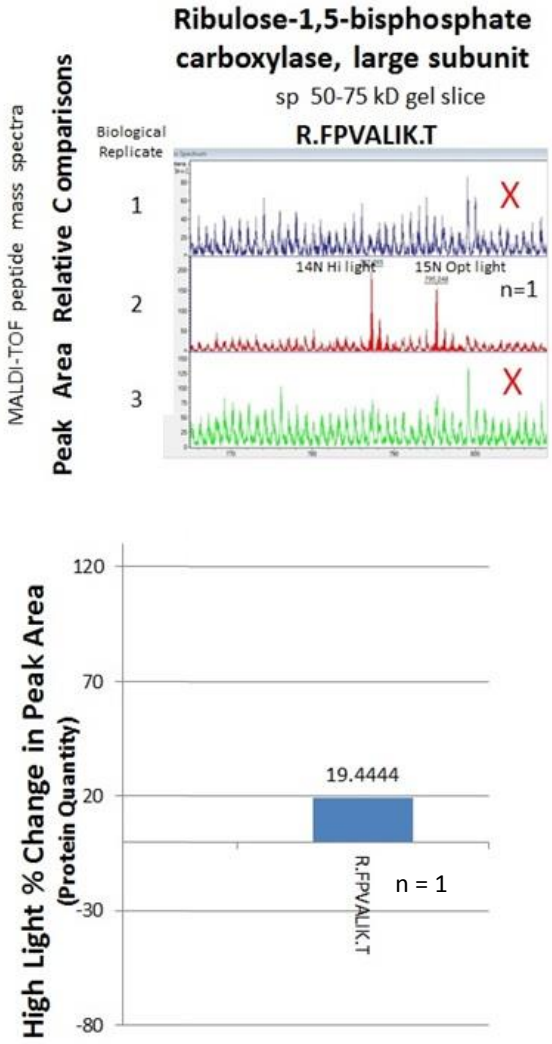

Figure 10. Ribulose-1,5-bisphosphate carboxylase, large subunit quantitative light- and heavy-peptide peak area comparisons from MALDI-TOF MS spectra. Peptides that were detected and analyzed were cross-identified from ESI-Ion trap MS^2 data. Spectra are shown for the peptide from all three biological replicates sampled. Red "X"s indicate biological replicates with poor peak resolution that were excluded from the statistical analyses. n = 1, so no t-tests were performed. The bar graph shows percent change in the peptide and corresponding protein level in the high-light relative to optimal light cultures from one biological replicate. Because matched peptides from both culture conditions (^{14}N high- vs ^{15}N optimal-light) were compared, the changes in peak area signal intensities may provide relative protein quantification. sp refers to the soluble protein fraction.

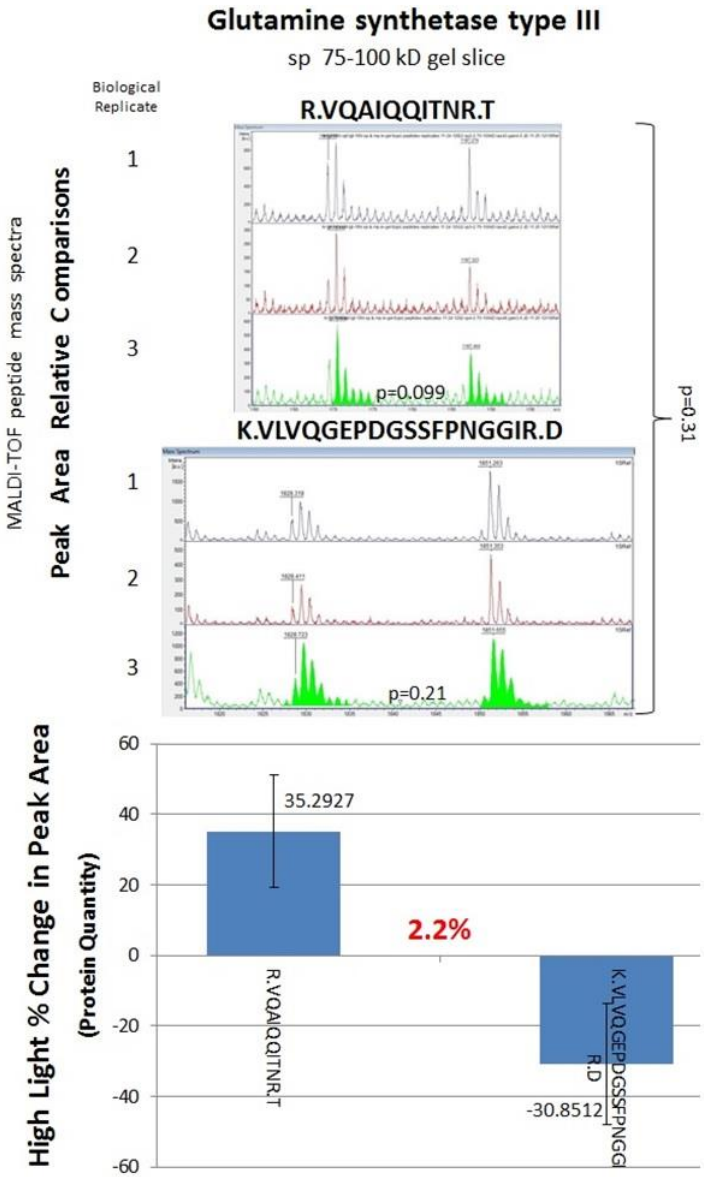

Figure 11. Glutamine synthetase type III quantitative light- and heavy-peptide peak area comparisons from MALDI-TOF MS spectra. Peptides that were detected and analyzed were cross-identified from ESI-Ion trap MS^2 data. Spectra are shown for the peptides from all three biological replicates sampled. All t-tests are paired, and the vertical t-test includes both peptides (and replicates) for the same protein. The bar graph shows the percent changes in the peptide and corresponding protein levels in the high-light relative to optimal light cultures from all three biological replicates. Because matched peptides from both culture conditions (^{14}N high- vs ^{15}N optimal-light) were compared, the changes in peak area signal intensities may provide relative protein quantification. The percent change in red is the average of the two peptide data for the given protein. sp refers to the soluble protein fraction.

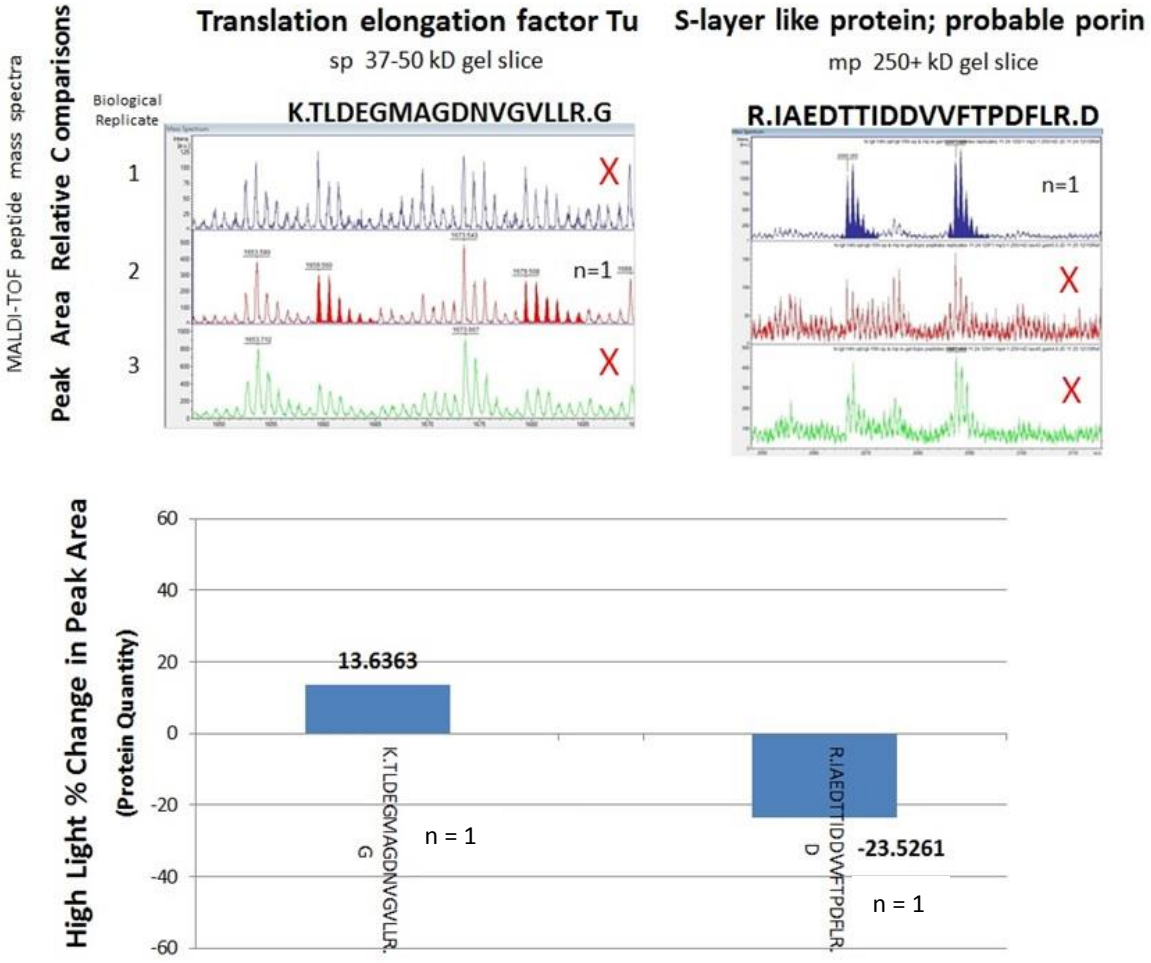

Figure 12. Translation elongation factor Tu and S-layer like protein quantitative light- and heavy-peptide peak area comparisons from MALDI-TOF MS spectra. Peptides that were detected and analyzed were cross-identified from ESI-Ion trap MS^2 data. Spectra are shown for the peptides from all three biological replicates sampled. Red "X"s indicate biological replicates with poor peak resolution that were excluded from the statistical analyses. n = 1 spectrum for each peptide, so no t-tests were performed. The bar graph shows the percent changes in the peptides and corresponding protein levels in the high-light relative to optimal light cultures from one biological replicate each. Because matched peptides from both culture conditions (^{14}N high- vs ^{15}N optimal-light) were compared, the changes in peak area signal intensities may provide relative protein quantification. sp and mp refer to the soluble and membrane protein fractions, respectively.

Discussion

Metabolic labeling of *Synechococcus* 7002 cells by substituting ^{15}N-$NaNO_3$ in the growth medium in place of ^{14}N-$NaNO_3$ is a simple and effective strategy for isotopic labeling of proteins. By mixing ^{14}N/^{15}N cells from different cultures that were grown identically with the exception of the variables tested, here high- versus optimal-light intensity, matched isotopically-shifted ^{14}N/^{15}N peptides could be compared and analyzed in the same mass spectrometry sample and instrument injection. This readily allows for signal detection of both ^{14}N and ^{15}N variants of otherwise identical peptides from the two culture conditions within the same dataset, and avoids normalizations and comparisons between separate MS-instrument runs. Since the ^{14}N/^{15}N peptides vary by only slight isotopic *m/z* shifts, they are detected as nearby ion pairs within the same MS spectrum. This facilitates relative protein quantification within the same MS-instrument run, since matching ^{14}N/^{15}N peptide pairs have the same amino acid chemistries, and thus instrument ionization efficiencies and signal intensities that are directly proportional to the peptide abundance; so that relative changes in the ^{14}N/^{15}N peptide pair signal intensities reflect changes in the ^{14}N/^{15}N peptide abundance that arise from the different culture conditions.

The ^{14}N/^{15}N metabolic-labeling approach also accounts for variations that may arise from the extensive sample processing required for mass spectrometry (cell lysis, ultracentrifugation, protein precipitation, denaturation, SDS-PAGE, trypsin-digestion, and desalting/purification), since the ^{14}N/^{15}N cell samples are mixed prior to these steps,

and processed concomitantly. This is in contrast to the tandem mass tag (TMT) labeling approach conducted in *Synechococcus* 7002 by Xiong *et al.* [15], where the final tryptic peptides underwent isobaric, multiplexed TMT-labeling separately after these sample processing steps. With the TMT-labeling, the bonded peptide mass reporters are cleaved during the tandem MS fragmentation, allowing for detection and relative quantification of the isotopic peaks during the tandem MS^2 analyses. However, with this TMT labeling methodology, rigorous controls must be performed to ensure that the sample processing and TMT labeling steps are performed consistently, efficiently, and are unbiased between the different samples and conditions being tested.

Standard, tandem mass spectrometry (MS/MS or MS^2)-based proteomic analyses favor detection of the most abundant proteins in a biological sample, because the automated ion selection in these methods is required for ion fragmentation and MS^2 analyses to obtain amino acid sequence data for peptide/protein identification. In *Synechococcus* 7002, abundant photosystem and phycobilisome proteins were predominantly detected. Optimization of MS instrumentation can improve sensitivity for less abundant proteins. Slower HPLC flow rates of ≤ 2 µl/min instead of 5-10 µl/min can improve proteome coverage, and newer mass spectrometers are coupled to nano-flow instead of micro-flow HPLC. Repeated injections of the same sample, analyzed over numerous small *m/z* ranges, without the use of automated ion selection, can also improve MS-based proteome coverage [22, 23]. However, this approach requires numerous, *e.g.* 30 or more, sample injections over a total instrument analysis time of three to five days, and is thus less commonly used. This approach may be possible with the *Synechococcus*

7002 soluble protein fraction, which provides a larger total sample volume (relative to membrane protein fractions) required for the repeated MS injections. In addition, MS instrument-based dynamic exclusion of abundant ions could be employed to improve proteome coverage. This approach may be particularly useful for the *Synechococcus* 7002 membrane fraction, which provides a smaller protein sample volume, where repeated sample injections are not readily feasible.

Sample pre-fractionation via chromatography and/or SDS-PAGE can also improve proteome coverage, as well as depletion of abundant proteins. SDS-PAGE of the *Synechococcus* soluble fraction resulted in a more diverse complement of MS^2-based protein identifications, relative to MS^2-analyses of the same sample in the absence of SDS-PAGE. A room temperature ultracentrifugation step to deplete some of the abundant phycobiliproteins (PBS) was also attempted, based on a brief method described in a protocol in our laboratory. But the protocol required further optimization, and publications related to trouble-shooting the method were elusive. Future MS^2-based proteomic analyses of *Synechococcus* soluble protein fractions would likely benefit from an optimized version of a PBS depletion protocol to improve the sensitivity of detection for other, much less abundant soluble proteins.

Most of the abundant and readily detected *Synechococcus* phycobilisome and photosystem proteins decreased under high-light growth relative to optimal-light conditions. This is consistent with the results of Xiong *et al.* [15], who quantified *Synechococcus* sp. PCC 7002 high-light protein levels via TMT-labeling and tandem

mass spectrometry. The consistent finding of decreased light-harvesting and photosynthesis protein content by two different MS-based protein quantification methods (TMT-labeling and the metabolic labeling reported here) reinforces the importance of this adaptation for these cyanobacteria. Interestingly, the RNA sequencing results of Xiong *et al.* [10] and Ludwig and Bryant [24] found that PS II transcripts increased in response to high light, whereas both the current data and those of Xiong *et al.* showed that the corresponding PS II protein levels decreased. A possible explanation is that mRNA transcript levels for photosynthesis proteins increase at high light intensity to meet the demands of high protein turnover resulting from increased levels of reactive oxygen species. Overall photosynthesis protein content may be regulated at a lower level to minimize over-absorption of excess light energy and production of oxygen radicals. Regardless, the disconnect between the mRNA and protein data reinforces the importance of dual transcriptomic and proteomic methodologies, to fully understand the cellular biology, particularly regarding differential RNA and protein stabilities.

Perhaps the high light decrease in *Synechococcus* phycobilisome and photosystem proteins is a biochemical regulatory mechanism of the photosynthetic activity to maintain redox equilibrium and prevent the extreme high light input from overcharging the electron transport chain leading to increased reactive oxygen species production. If high light intensity is consistently available, it is reasonable to assume that fewer light harvesting proteins are needed to maintain electron transport and redox equilibrium. This is generally consistent with findings from a variety of photosynthetic organisms [25] [26]. In contrast, in consistently low-light environments increased light-harvesting proteins

would be advantageous to capture all available photons, and this has been demonstrated in some marine cyanobacteria [27]. In contrast to environments with stable illumination, many natural environments are subjected to extreme rapid fluctuations in light intensity that pose special hazards. Organisms in these environments have evolved a variety of rapid-response mechanisms including state transitions, alternative electron transfer pathways, and energy-dissipating non-photochemical quenching mechanisms to excess photon absorbance and damaging overreduction of electron transport [28]. In connection to its environment and related evolutionary pressures, perhaps the *Synechococcus* 7002 high-light protein level adaptions have been influenced by its aquatic, equatorial environment of Puerto Rican mud flats. This environment may be subject to transient solar light focusing and polarizations caused by the shallow water and wave surfaces which could cause variations in light intensities [29]. Additionally, since evidence of cyanobacterial life is dated as early as 3000 million years ago [30], these organisms may have experienced temporal fluctuations in solar radiation, further influenced by variations in the atmosphere's transparency and composition (*e.g.*, ozone and particulates) over time [31].

Overall, the $^{14}N/^{15}N$ peak area comparisons for relative protein quantification were quite consistent among biological replicates and peptides for the same protein. One outlier was the smallest sequenced peptide R.ALELAFR.H for phycobilisome (PBS) core-membrane linker ApcE (Figure 4C). While the other replicate detected peptides for PBS core-membrane linker ApcE showed consistent, significant high-light decreases of 53.4%, 42.2%, and 62.3% (at $p = 0.015$), R.ALELAFR.H showed an increase of 77.1%

in high light, although not significantly so because of the large signal variance among biological replicates ($p = 0.075$). This unexpected, apparent increase in high-light abundance may be related to the small size of R.ALELAFR.H. This short amino acid sequence may be a common degradation product of PBS core-membrane linker ApcE, or perhaps this peptide is highly stable. Indeed, the *Synechococcus* sp. PCC 7002 high-light adaptative model proposed by Xiong *et al*. included degradation of the phycobilisomes, and PBS degradation has also been described for other cyanobacterial nutrient-starvation (C, N, P, S, and Fe) stress conditions [32] [33].

Since R.ALELAFR.H is one of the smallest peptide sequences detected overall, it could also be inaccurately assigned to PBS core-membrane linker protein ApcE. If this small peptide sequence is not unique to ApcE, then it could originate from an unknown protein, whose level increases in response to high light intensity. However, several online NCBI BLAST searches of the sequence against the protein sequence databases of *Synechococcus* sp. PCC 7002 and related organisms resulted in no substantial matches with any other proteins besides PBS core-membrane linker protein ApcE. Thus incorrect protein assignment is unlikely in this case. However, a future consideration could be utilizing a minimum peptide sequence length as a threshold for inclusion in the final protein quantification calculations.

Another interesting variation in the $^{14}N/^{15}N$ peak area comparisons for relative protein quantification, was observed for peptide R.LVPDKGQLGFR.F for PS I P700 chlorophyll A apoprotein A1 (Figure 4A). When detected in the high-molecular-weight

250+ kD gel slice, a significant decrease of 63.1% ($p = 0.023$) was observed. When detected in a different 55-100 kD gel slice, the same peptide showed no significant difference in abundance in high- relative to optimal light (+2.1%, $p = 0.39$). This may have resulted from incomplete denaturation of photosynthesis protein complexes during SDS-PAGE. The 250+ kD gel slice included visible, intact photosystem complexes that were not fully SDS-denatured, and this could reflect a more accurate ratio of the proteins in still intact PS I complexes. This is supported by the other PS I proteins detected in the same 250+ kD gel slice, which showed similar decreases of 68.5% and 68.2% ($p = 0.021$ and 0.0097) in the high light cultures. Alternatively, incomplete denaturation of photosynthesis complexes may have led to selective or differential separation of certain polypeptide subunits but not others in the protein complexes obtained from high-light relative to optimal-light cultures. Such selective separation of proteins could lead to over or under estimation of the abundance of the separated proteins. For future $^{14}N/^{15}N$ metabolic-labeling proteomic experiments with *Synechococcus* sp. PCC 7002 or other cyanobacteria, it may be useful to try native-PAGE for separating intact protein complexes for improved protein quantification.

Concluding Remarks

With a fully-sequenced and transformable genome, *Synechococcus* sp. PCC 7002 is an excellent model organism and host platform for investigating photosynthesis and prokaryotic circadian rhythms, and for bioproduction applications. Data presented here

demonstrate that $^{14}N/^{15}N$ metabolic-labeling coupled with MALDI-TOF MS and ESI Ion-Trap MS^2 comprise a valuable proteomic approach for gaining insight into protein responses and adaptation of *Synechococcus* sp. PCC 7002 and other cyanobacteria to changes in culture and environmental conditions. Full sunlight is a critical stress condition faced by photosynthetic organisms, and understanding biological responses and adaptations to it will be essential for large-scale development of microalgae for bioproducts/biofuels production. *Synechococcus* sp. PCC 7002 is of particular interest in this regard because it tolerates extreme, high light intensities of at least twice full sunlight (4500 µmol photons m^{-2} s^{-1}) that are lethal to many algae. Work presented here in this thesis shows that downregulation of light-harvesting and photosynthesis proteins is part of the adaptive mechanism that allows these cyanobacteria to thrive at high light intensities. Similar approaches with current, state-of-the-art mass spectrometers would enable much deeper analysis of proteome responses including that would include much less abundant proteins that may have important regulatory roles.

References

1. Batterton, J.C., Jr. and C. Van Baalen, *Growth responses of blue-green algae to sodium chloride concentration.* Arch Mikrobiol, 1971. **76**(2): p. 151-65.
2. Stevens, S.E. and R.D. Porter, *Transformation in Agmenellum quadruplicatum.* Proc Natl Acad Sci U S A, 1980. **77**(10): p. 6052-6.
3. Essich, E., S.E. Stevens, Jr., and R.D. Porter, *Chromosomal transformation in the cyanobacterium Agmenellum quadruplicatum.* J Bacteriol, 1990. **172**(4): p. 1916-22.
4. Nomura, C.T., T. Sakamoto, and D.A. Bryant, *Roles for heme-copper oxidases in extreme high-light and oxidative stress response in the cyanobacterium Synechococcus sp. PCC 7002.* Arch Microbiol, 2006. **185**(6): p. 471-9.
5. Barber, J. and B. Andersson, *Too much of a good thing: light can be bad for photosynthesis.* Trends Biochem Sci, 1992. **17**(2): p. 61-6.
6. Zhu, Y., et al., *Roles of xanthophyll carotenoids in protection against photoinhibition and oxidative stress in the cyanobacterium Synechococcus sp. strain PCC 7002.* Arch Biochem Biophys, 2010. **504**(1): p. 86-99.
7. Kirilovsky, D., *Photoprotection in cyanobacteria: the orange carotenoid protein (OCP)-related non-photochemical-quenching mechanism.* Photosynth Res, 2007. **93**(1-3): p. 7-16.
8. Kim, J.H. and K.H. Suh, *Light-dependent expression of superoxide dismutase from cyanobacterium Synechocystis sp. strain PCC 6803.* Arch Microbiol, 2005. **183**(3): p. 218-23.
9. Helman, Y., et al., *Genes encoding A-type flavoproteins are essential for photoreduction of O2 in cyanobacteria.* Curr Biol, 2003. **13**(3): p. 230-5.
10. Campbell, D., et al., *Chlorophyll fluorescence analysis of cyanobacterial photosynthesis and acclimation.* Microbiology and Molecular Biology Reviews, 1998. **62**(3): p. 667-+.
11. Anderson, J.M., Y.I. Park, and W. Chow, *Photoinactivation and photoprotection of photosystem II in nature.* Physiol Plant, 1997. **100**: p. 214-223.
12. Keren, N., et al., *Mechanism of photosystem II photoinactivation and D1 protein degradation at low light: The role of back electron flow.* Proceedings of the National Academy of Sciences of the United States of America, 1997. **94**(4): p. 1579-1584.
13. Cameron, J.C. and H.B. Pakrasi, *Essential role of glutathione in acclimation to environmental and redox perturbations in the cyanobacterium Synechocystis sp. PCC 6803.* Plant Physiol, 2010. **154**(4): p. 1672-85.
14. van Thor, J.J., et al., *Light harvesting and state transitions in cyanobacteria.* Botanica Acta, 1998. **111**(6): p. 430-443.
15. Xiong, Q., et al., *Integrated transcriptomic and proteomic analysis of the global response of Synechococcus to high light stress.* Mol Cell Proteomics, 2015. **14**(4): p. 1038-53.
16. Lundgren, D.H., et al., *Role of spectral counting in quantitative proteomics.* Expert Rev Proteomics, 2010. **7**(1): p. 39-53.
17. Thompson, A., et al., *Tandem mass tags: a novel quantification strategy for comparative analysis of complex protein mixtures by MS/MS.* Anal Chem, 2003. **75**(8): p. 1895-904.

18. McAlister, G.C., et al., *Increasing the multiplexing capacity of TMTs using reporter ion isotopologues with isobaric masses.* Anal Chem, 2012. **84**(17): p. 7469-78.
19. Pandhal, J., et al., *A cross-species quantitative proteomic study of salt adaptation in a halotolerant environmental isolate using 15N metabolic labelling.* Proteomics, 2008. **8**(11): p. 2266-84.
20. Baran, R., et al., *Metabolite identification in Synechococcus sp. PCC 7002 using untargeted stable isotope assisted metabolite profiling.* Anal Chem, 2010. **82**(21): p. 9034-42.
21. Candiano, G., et al., *Blue silver: a very sensitive colloidal Coomassie G-250 staining for proteome analysis.* Electrophoresis, 2004. **25**(9): p. 1327-33.
22. Panchaud, A., et al., *Precursor acquisition independent from ion count: how to dive deeper into the proteomics ocean.* Anal Chem, 2009. **81**(15): p. 6481-8.
23. Panchaud, A., et al., *Faster, quantitative, and accurate precursor acquisition independent from ion count.* Anal Chem, 2011. **83**(6): p. 2250-7.
24. Ludwig, M. and D.A. Bryant, *Transcription Profiling of the Model Cyanobacterium Synechococcus sp. Strain PCC 7002 by Next-Gen (SOLiD) Sequencing of cDNA.* Front Microbiol, 2011. **2**: p. 41.
25. Hassidim, M., et al., *Acclimation of Synechococcus strain WH7803 to ambient CO2 concentration and to elevated light intensity.* Journal of Phycology, 1997. **33**(5): p. 811-817.
26. Horton, P., A.V. Ruban, and R.G. Walters, *Regulation of light harvesting in green plants.* Annual Review of Plant Physiology and Plant Molecular Biology, 1996. **47**: p. 655-684.
27. Garczarek, L., et al., *Multiplication of antenna genes as a major adaptation to low light in a marine prokaryote.* Proceedings of the National Academy of Sciences of the United States of America, 2000. **97**(8): p. 4098-4101.
28. Scheibe, R., et al., *Strategies to maintain redox homeostasis during photosynthesis under changing conditions.* J Exp Bot, 2005. **56**(416): p. 1481-9.
29. Cronin, T.W. and N. Shashar, *The linearly polarized light field in clear, tropical marine waters: Spatial and temporal variation of light intensity, degree of polarization and e-vector angle.* Journal of Experimental Biology, 2001. **204**(14): p. 2461-2467.
30. Schopf, J.W., *Fossil evidence of Archaean life.* Philosophical Transactions of the Royal Society B-Biological Sciences, 2006. **361**(1470): p. 869-885.
31. Wild, M., et al., *From dimming to brightening: Decadal changes in solar radiation at Earth's surface.* Science, 2005. **308**(5723): p. 847-850.
32. Richaud, C., et al., *Nitrogen or sulfur starvation differentially affects phycobilisome degradation and expression of the nblA gene in Synechocystis strain PCC 6803.* Journal of Bacteriology, 2001. **183**(10): p. 2989-2994.
33. Sherman, D.M. and L.A. Sherman, *Effect of Iron-Deficiency and Iron Restoration on Ultrastructure of Anacystis-Nidulans.* Journal of Bacteriology, 1983. **156**(1): p. 393-401.